CHAPTER

2

An "Anthropically" Flavored Look at Some Basic Aspects of NMR Spin Physics Using a Classical Description

Csaba Szántay, Jr.

Gedeon Richter Plc, Spectroscopic Research Division, Budapest, Hungary

OUTLINE

2.1 INTRODUCTION

The main aim of Part II is to illustrate AA "at work" in why-science via three selected topics drawn from basic (liquid-state) NMR theory, as discussed in Chapters 2–5. As a preliminary thought, it must be stressed that NMR theory is an awesome depository of great intellectual feats and a testament to brilliant scientific thinking. However, NMR theory has its own very interesting Delusors which have created some widespread misconceptions about the physical essence of some basic NMR phenomena. In that regard, NMR theory is remarkably well suited for an AA-conscious scrutiny: it is an intriguing intellectual "brew" of quantum

Anthropic Awareness
http://dx.doi.org/10.1016/B978-0-12-419963-7.00002-X

mechanics, classical physics, mathematical and physical descriptions, and pictorial models, from all of which several Delusors and unsound models have stemmed (note again that, as expressed in the Preface, this should not be understood as a derogatory statement). Part II aims to demonstrate that when NMR theory is examined (or more precisely: when it is dared to be examined) with an AA mentality, these false ideas can come to light and can open the way to some truly instructive and revealing insights into the Mental Traps behind those misconceptions and the way things should be interpreted correctly (cf. Chapter 1, Pillars 14 and 15). In that regard, we must first and foremost clarify the aims, the scope, and the internal technical "design" of Part II.

This chapter has a triple goal. On the one hand it aims to offer the essential technical background (the bare necessities) that will be needed for the reader to better appreciate the subsequent topics laid out in Chapters 3–5. However, the following discourse is *not* intended to *explain* basic NMR theory in any extensive or technically rigorous manner. NMR theory, even *basic* NMR theory, is a staggeringly huge subject which has been extensively, thoroughly, and eminently explored in the scientific literature over about the last seven decades. Thus, attempting any thematic and self-contained treatment of NMR theory would not only be pointless, but also hopeless, and would derail us from the main theme of this book. I am therefore forced to assume that the reader has had at least a minimum exposure to NMR theory, and so he has *some* idea of the basic concepts of the nuclear magnetic resonance phenomenon and Fourier-transform NMR spectroscopy (such as spin, Larmor precession, macroscopic magnetization, relaxation, excitation by a radio-frequency (RF) pulse, free-induction decay (FID), chemical shift, scalar, and dipolar coupling, etc.). On the other hand, with this chapter I not only want to give the necessary technical preliminaries for the subsequent chapters, but by tacitly building on this presumed prior NMR knowledge of the reader, I want to portray those basic concepts with a certain degree of AA "flavor" attached to them, thus hoping to present them in a different light. This should bring the reader into an AA-conscious "NMR-theory-mood," also offering a kind of initiation into NMR from an AA perspective. Thirdly, this chapter is written also with a view to preparing the reader for Chapter 7 which reviews the NMR techniques used in the structure-elucidation examples of Part III.

Having presented the basics in this chapter, Chapters 3–5 will address the following three topics: (1) the flaws of the famous two-cone model of NMR; (2) the myth of Heisenberg's Uncertainty Principle being responsible for a monochromatic RF pulse's ability to excite a broad spectrum of resonance frequencies; (3) the myth that NMR excitation is caused by a physically existent rotating magnetic component of the linearly oscillating RF excitation field that elicits the NMR response.

In the spirit of this book, throughout Part II we will try to be as nontechnical as possible; in fact, we expressly want to present a largely qualitative and *synoptic* explanation of NMR phenomena (cf. Pillars 6 and 7). This is a point of much importance for two interlocking reasons. First, it means that we will make several statements without proof or a deeper explanation, expecting that they should be accepted "at face value," but with the understanding that the technical background behind those statements is available either in the majority of general NMR textbooks or in the specific literature cited herein in connection with those statements. Second, "going synoptic" reflects an approach that is seldom practiced in the literature, be it technical or educational. However, as discussed in Pillar 6, a healthy synoptic understanding does not automatically emerge from having thoroughly studied the technical details. In fact,

becoming drenched in technical detail may actually create a "not-seeing-the-forest-for-the-trees" effect, inhibiting one from attaining a proper synoptic apprehension of a topic (see Trap #15). We will go the other way round and try to approach the pertinent technicalities as synoptically as possible. That being said, some technicalities will unavoidable emerge (especially in Chapter 4), driven by a need to phrase certain concepts as accurately as possible, which sometimes requires exquisite mathematical expressions.

Finally, I must comment on the *significance* of understanding and correcting the flaws brought to attention in Chapters 3–5. Although each of those flaws represents a scientifically incorrect description of the physical world, the flaws are such that they have no or little *practical* implications. In fact, many NMR spectroscopists have been doing excellent science in theoretical and methodological NMR in spite of holding these misconceptions. So what is the scientific merit of addressing such flaws? As already argued in Pillar 15, although it makes no practical difference in our daily lives whether the Sun moves around the Earth or vice versa, it *does* make a difference whether we are under the *illusion* that the former is true, or we *know* that actually the latter is true. For entirely analogous reasons, it *does* make a difference whether our understanding of the physical world rests on provably erroneous models or on scientifically validated descriptions, even if this difference has no particular practical consequence that we can think of at this time. Illusions of understanding (cf. Pillar 5) should not be tolerated by science, and, as argued in Pillars 14, 15, and 18, uncovering and refuting Delusors is a legitimate, instructive, and inspiring scientific endeavor.

Finally, the technical framework (the "contextual space") as well as the scope of our discussion should be defined.

As for the technical framework, by default we will restrict ourselves to consider a liquid-state ensemble of identical spin-1/2 nuclei (see below) with a positive gyromagnetic ratio (see below), placed in a strong homogeneous static magnetic field. We assume that the spins are noninteracting or are only very weakly interacting with each other and with the environment (the "lattice"). The interaction being very weak means that the energy of the system can, to a very good approximation, be regarded as the sum of the energies of the individual spins, and in that respect the interaction energy can be ignored. However, the interaction energy is still large enough so that spins that happen to be sufficiently close to each other can "feel" each other's presence and can therefore exchange energy; this assumption is needed to explain relaxation phenomena. The number of spins in the ensemble is assumed to be very large, of the order of Avogadro's number. In practice, such a system is approximated, for example, by the protons in a sample of about 1 μl of pure water. In the following, when talking about an "ensemble of spins," I will implicitly mean an ensemble having the above features and I will use the terms "proton" and "spin" interchangeably. For simplicity, I will also assume that the T_1 and T_2 relaxation times (see below) of the nuclei are equal and are on the order of seconds. Thus, during excitation by a hard RF pulse which is on the order of microseconds, relaxation effects can be ignored.

As for the scope, when talking about basic NMR theory it is important to appreciate that the basic NMR phenomenon has two interrelated facets: excitation and relaxation. Both are inherent to NMR and are equally important, and both aspects have their own technical intricacies. Herein, because of the examples presented in Part II, we will mostly be concerned with the excitation part, but some attention will also be devoted to relaxation.

In what follows I will put emphasis on the *classical* description of a single spin and a spin ensemble, which will also prove to serve as a handy reference for the arguments in the

subsequent chapters. Only marginal comments will be made on the quantum-mechanical description of NMR so as to serve as a transition into Chapter 3 which will unfold this topic more fully.

2.2 INTRODUCTORY THOUGHTS ON THE CHARACTERISTICS OF NMR THEORY

In order to take what I think is a "healthy" mental attitude toward NMR theory, as well as to prepare for recognizing some of its Delusors, the very first thing that one needs to see clearly is that NMR phenomena lend themselves to be treated both classically and quantum-mechanically. This is a centrally important aspect of NMR theory which is known by all NMR spectroscopists because it is an inescapable feature of the NMR literature. However, many delicacies ensuing from this duality are not addressed in the basic NMR literature or are treated in a rather sketchy way, resulting in various misconceptions. The subtleties of this situation stem from the fact that while the physics of NMR is fundamentally grounded in the quantum-physics of atomic-scale (often also called microscopic-scale) nuclear magnets, in reality NMR spectroscopy always measures the behavior of the *macroscopic* bulk magnetization produced by *ensembles* of noninteracting or weakly interacting nuclear magnets. That macroscopic behavior can be treated both quantum-mechanically and classically, but the latter is often simpler and intuitively more accessible, which is a rather important trait with regard to the way scientists understand and think creatively about a phenomenon (cf. Pillars 11 and 12). (As it will be further expounded below, it is an intriguing aspect of NMR theory that some *unsound* (i.e., misleading—cf. Pillar 13), simplified quantum-mechanical descriptions appear to be simple, convincing, and intuitively accessible, while *sound* quantum-mechanical descriptions can be very complicated; it is with respect to the latter that a sound classical description is simple). One should make note here of the famous Correspondence Principle which, in essence, states that the phenomenological quantum-mechanical description of a large collection of identical and noninteracting atomic entities gives the same result as the classical description of that ensemble. Thus, the phenomenon that an ensemble of nuclear magnetic moments can be made to "resonate" when placed in a strong static magnetic field and subjected to a weak alternating magnetic field should, as pointed out by Hanson,[1] not even be called a quantum effect if by "quantum effect" we mean such phenomena that can *only* be described correctly by quantum-mechanical means, and a classical-physical treatment fails. Nevertheless, certain NMR phenomena (such as the nuclear Overhauser effect (NOE) or *J*-coupling effects) can typically be more conveniently treated by quantum-mechanical tools.

Yet another feature of NMR worth keeping in mind is that it is often easier to devise mathematical expressions that describe NMR phenomena rather well than to understand the physics behind the mathematics (cf. Pillar 6, Trap #11). In fact, it is notoriously difficult to gain a sound *physical* picture of the spin-world in NMR, and it is quite intriguing to observe how differing NMR spectroscopists can be in their personal conceptualization of even the most fundamental physical aspects of NMR.

Grasping and dealing with this blend of quantum-mechanical and classical descriptions, and mathematical and physical understanding, is not easy. We have been accustomed to the

way classical mechanics is applied to describing the behavior of macroscopic material objects that are a part of our "everyday" world as we know it through our normal human perception. Although we know that those objects are built from atoms, and that *in principle* their macroscopic behavior could be calculated by calculating (quantum-mechanically) the behavior of the individual atoms and summing up the results (albeit this would be exceedingly complicated), we normally ignore this atomic and humanly imperceptible aspect of the object, and just deal directly with its macroscopic feature in terms of classical mechanics. In this case, the distinction between the macroscopic and atomic aspects of the object is trivial because these are so *distant* from each other in terms of size and human perception. However, the macroscopic and atomic aspects of an ensemble of nuclear magnets are much *closer* to each other. On the one hand, the macroscopic magnetization is not more directly accessible to human perception than its constituent atomic magnets. On the other hand, the macroscopic magnetization is a somewhat tricky concept hovering between physical reality and abstraction: although it is convenient to think about it as a vector (see below) which rotates, precesses, and changes its length in all sorts of complicated and wonderful ways in an NMR experiment, and we know that it is this bulk behavior that we measure physically, we also know that it is actually the individual nuclear magnetic "vectors" that "resonate" and not their mathematical vector sum; thus, in this case it is more difficult to ignore the atomic aspect of the macroscopic magnetization when we want to find or understand classical models that describe the behavior of the latter.

For all the above reasons, the classical and quantum-mechanical treatments of NMR are closely intertwined, so we can look upon NMR from two different perspectives: with a classical-physical "eye" and with a quantum-mechanical "eye." NMR spectroscopy involves a plethora of phenomena that derive from the basic magnetic resonance phenomenon, and sometimes it is the classical-physical, and sometimes the quantum-mechanical approach that proves more *convenient* for describing these phenomena. Personal technical "tastes" and background schooling also matter: some authors prefer to use classical methods (sometimes seemingly at all costs), while others take a similar attitude toward using quantum mechanics. This is probably best attested to by the seminal papers of Bloch et al. and Purcell et al. in which they independently and simultaneously described the discovery and theoretical rationalization of the basic NMR phenomenon in 1946, thereby launching NMR onto its incredibly successful orbit of development.[2,3] Bloch treated NMR essentially from a classical point of view, thinking of nuclear magnets as tiny resonators which precess about the static magnetic field, yielding a bulk polarization whose orientation can be changed by an oscillating magnetic field, while Purcell viewed the phenomenon as stemming from transitions induced by the oscillating field between nuclear quantum states that emerge in a static magnetic field. The two groups conceptualized the NMR phenomenon so differently that it actually took some time for both of them to realize that they were describing essentially the same phenomenon.[4]

This duality is one of the beauties of NMR theory. It is also one of its evils. It is a beauty so long as someone understands the technical essence of these binary approaches to NMR and has the faculty of distinguishing between scientific descriptions and reality (cf. Pillars 2 and 3). NMR, as a collection of various phenomena and various descriptions of those phenomena, can be thought of as a "patchwork" of different quantum-mechanical and classical models that partly overlap and are partly distinct. NMR theory offers a wonderful intellectual experience if one understands models for what they are (cf. Pillar 13), does not get overly

submerged within a given model, does not confuse models with reality (Trap #18), is aware of the contextual spaces of models (Traps #19 and #20), and can flexibly "move" mentally between them when contemplating NMR phenomena. NMR theory is a remarkable test of these faculties. On the other hand, the classical-physical and quantum-mechanical duality of NMR can be a source of many Mental Traps (as will be discussed below) if their distinction is blurred or unsoundly merged (as it is the case in several basic treatments of NMR) and the faculty of model-oriented thinking is absent.

Besides this fundamental duality, NMR theory has some other "anthropically" relevant aspects that should be emphasized right from the start rather than letting them either transpire gradually from a prolonged study of NMR, or, worse (but typical), not to transpire at all. NMR is about the behavior of nuclear spins (atomic-scale angular momenta) and the associated magnetization of atoms (the magnetic moments). The concept of spin (and therefore that of the magnetic moment) is highly elusive, although it is often treated illusively simply (see more on this below). What we can do is to use abstract mathematical symbols and equations to describe the spin, and to validate the mathematics by experiment. The nonpictorial mathematical descriptions that have been formulated to that effect work nicely, but the human mind naturally strives to "morph" these abstract concepts into a more physical understanding (cf. Pillar 6), typically in the form of pictorial representations that will help one to think and talk about NMR phenomena in terms of a physically tangible geometrical model (cf. Pillars 11 and 12). However, the origin and quantum-mechanical behavior of the spin are so mysterious and so unlike anything that our mind has been conditioned to apprehend in our macroscopic world, that the true physical understanding of spin seems to be beyond the scope of the human mind's apperception. Thus, the ensuing pictorial representations are quite dubious and have certain properties that must be well understood and always kept in mind: (a) It is impossible to represent physical "spin-reality" in an entirely satisfactory pictorial form, and therefore such images are always more or less skewed. (b) All such pictures are *metaphoric* models (cf. Pillar 10). (c) Within the context of (a) and (b) these pictorial models can be *sound* or *unsound* (cf. Pillar 13). (d) A sound pictorial model, albeit not a correct representation of physical "spin-reality," can be very useful in *thinking* about that reality. (e) An unsound pictorial model of spins acts as a powerful Delusor because, although misleading, it *seems* to provide a convincing visual imagery of reality itself (cf. Trap #16).

Although, as we will see, several Mental Traps contribute to the widespread misconceptions that exist about the physical essence of NMR, as a part of the initial mindset with which I encourage the reader to approach the whole topic, I want to put particular emphasis on the Traps associated with our tendency to muddle the difference between mathematical and physical descriptions (Traps #11-#13). Because of this, and in order to stress the importance of distinguishing between a mathematical and a physical understanding of the world (cf. Pillar 6), in the following discussion I will take special care to use a verbiage that reflects this difference and I encourage the reader to be sensitive about this.

Finally, I want to point out that in spite of the long history of NMR theory, and in spite of the fact that its mathematical apparatus is well worked out, we can still witness insightful discourses on the interpretation of its physical essence, often correcting widely held misconceptions. This shows that one should approach the basics of NMR with an inquisitive mind (Fig. 1.1) rather than with a default mindset that takes all statements for granted on the perceived precept that NMR theory represents vintage, and therefore proven (Trap #8), science.

In fact, searching for new and nonparadigmatic ways of looking at the basics can be a very revealing endeavor (cf. Pillars 16 and 17).

It is, then, with the above intellectual and emotycal attitude that one should (in my view) approach NMR theory in general, and the short discussion below in particular.

2.3 CLASSICAL PORTRAYAL OF AN INDIVIDUAL SPIN

With reference to the Correspondence Principle, the classical description of NMR fundamentally pertains *not* to the individual spins or magnetic moments $\boldsymbol{\mu}$, but to the *macroscopic magnetization* $\sum\boldsymbol{\mu} = \mathbf{M}$ of the spin ensemble and (more precisely, $\mathbf{M}$ is usually defined for the number of spins contained in a unit volume of sample, but we can ignore that nuance here). Bloch's original classical treatment of the NMR phenomenon via the famous Bloch equations reflects this stance: the equations describe the *phenomenological* behavior of the macroscopic magnetization without any attempt to rationalize that behavior in terms of microscopic considerations.[2]

The nuclear spin is a quantum-mechanical entity, and therefore any attempt to describe its physical behavior classically (as it is done in many of the established basic NMR textbooks) may seem like a strange idea, because we *know* that a single spin does *not* behave as a classical object. So why bother? As it turns out, we have two good reasons to do so. Although we cannot *a priori* be certain whether a classical description of a single spin's behavior in NMR will yield a sound or an unsound model (cf. Pillar 13), bestowing classical properties upon the spin is a natural attempt of the human mind to be able to *think* about a spin and a spin ensemble in a constructive manner (cf. Pillar 11). Indeed, there seems to be a very human need to formulate some idea about what kind of microscopic physical spin-behavior *causes* the macroscopic magnetization to move and change its length the way it does during an NMR experiment. If we approach the situation by deliberately thinking in terms of *metaphoric models* with well understood purposive infrastructures and contextual spaces, and if we are *aware* of the fact that in doing so we are not trying to rigorously emulate physical reality (cf. Pillars 10 and 13), we find that we can come up with a convenient and very helpful classical treatment of the individual spins and the associated $\boldsymbol{\mu}$ magnetic moments (see below). Although this approach is physically deceptive in the sense that it attempts to approximate a quantum-physical object (spin) with a classical-physical object (rotating magnetic dipole), it turns out to be mathematically justifiable from a quantum-mechanical viewpoint: quite amazingly, the quantum-mechanical expectation value $\langle\mu\rangle$ of the magnetic moment operator for a single spin obeys the classical equations (see Chapter 3)! Overall, the classical approach can be embraced as providing a sound metaphoric model which is a valid, useful, and human-mind-friendly pictorial representation of physical reality. Many descriptions of basic NMR portray the individual spin classically without pointing out the metaphoric nature of this model, thus muddling the difference between the classical and quantum-mechanical description and easily creating confusion between reality and the model (cf. Traps #18-#20).

To see how the classical approach works, we first need to review some classical-mechanical principles that may be applied to the individual spins. The classical approximation sets out by noting that certain so-called NMR-active nuclei (whose atomic number or mass number is odd, such as, e.g., ^{1}H or ^{13}C) exhibit the special property that they have an *angular momentum*.

As it is familiar from classical physics, the angular momentum **P** is a vector quantity (herein mathematical symbols set in nonitalicized bold denote vectors) which characterizes spinning objects and which is the product of the spinning body's moment of inertia (which is a measure of the object's resistance to changing its angular velocity) and its angular velocity **ω** (which is also a vector quantity because it specifies not only the velocity of the rotation but also its direction). For a body that rotates with a constant angular velocity $\omega = |\boldsymbol{\omega}|$ about a given axis, the direction of **P** gives the direction of the rotational axis *and* the sense of rotation about the axis (i.e., whether the body rotates "to the right" or "to the left" about the axis according to the famous right-hand rule), while its absolute value (magnitude) $P = |\mathbf{P}|$ is the larger the bigger is the mass and the rotational velocity of the rotating body. Those nuclei that possess an angular momentum may be intuitively conceptualized within this classical framework of description as tiny spinning tops, which is why the jargon refers to the angular momentum of such nuclei as "*spin*." Note however that in reality spin does *not* arise because of the actual rotation of the nucleus or the rotation of its constituent nucleons. Rather, spin is an intrinsic and very mysterious feature of atomic particles which is probably beyond the reach of human understanding.[5] Nevertheless, viewing nuclei as if they were tiny spinning tops is a useful metaphoric aid (cf. Pillar 10) so long as we do not confuse this image with reality (cf. Trap #18).

Nuclei also exhibit an intrinsic *permanent magnetism* (nuclear paramagnetism) which is closely related to spin and which is just as mysterious as spin (sometimes the magnetism of nuclei is rationalized as arising because every nucleus carries charges, and due to the nuclei's perceived spin, these charges will circulate about the **P** vector, generating, as is well known, a magnetic dipole along the direction of **P**; this picture however is incorrect: the magnetism of nuclei is not due to a circulating charge, it is just *there*[5]).

This nuclear magnetism of spin-possessing nuclei may be conceptualized classically as a tiny cylindrical bar magnet (a magnetic dipole) *spinning* about its major axis along the direction of **P**. Now, ignoring this spinning for a moment, magnetic dipoles are characterized by their *magnetic moment* **μ**, a vector quantity which serves to express the "vehemency" with which the dipole wants to align itself along the direction of a static homogeneous external magnetic field, the latter being represented by the magnetic induction vector **B**. More specifically, if we place the dipole **μ** in the static magnetic field of **B** induction such that **B** and **μ** enclose an arbitrary angle θ, then **B** will exert a torque

$$\mathbf{T} = \boldsymbol{\mu} \times \mathbf{B} \,(\text{i.e.}, T = \mu B \sin\theta) \tag{2.1}$$

on **μ**, and if the dipole is not spinning, this torque will act to rotate **μ** in the direction of **B** about an axis that is perpendicular to **μ** (excluding of course the situation when $\theta = 0$ and $\theta = \pi$, in which cases $T = 0$), just as a compass behaves. The magnitude of the magnetic moment ($\mu = |\boldsymbol{\mu}|$) can be measured by the magnitude of the torque ($T = |\mathbf{T}|$) acting upon it. However, the nuclear magnetic dipole that we are dealing with is *spinning*, and while this does not affect the above definition of magnetic moment as far as Eq. (2.1) and the magnitude μ are concerned, it does have a profound effect on how the dipole behaves under the action of the torque **T** (see below). It is therefore imperative that every time we see the symbol **μ**, we keep in mind that it represents a nuclear magnetic dipole that is spinning about the direction of **P**, that is, it is a magnetic moment with an angular momentum, in other words a *gyro*magnetic moment (the word "gyro" comes from the Greek word "turn"). The connection between the nuclear magnetic moment and the angular momentum (spin) is given by the equation

$$\boldsymbol{\mu} = \gamma \mathbf{P}, \tag{2.2}$$

where γ is the gyromagnetic ratio, a scalar constant that is characteristic of the atom type and may have a positive or negative sign. Note that for the case of the positive γ that we restrict our discussion to, the moment vector and the angular momentum vector (spin) point in the same direction (this is noted because it simplifies some aspects of the discussion). Although, strictly speaking, "spin" means "angular momentum," NMR people often use the word "spin" more informally to also imply the magnetic moment $\boldsymbol{\mu}$ on the basis of Eq. (2.2).

Yet another point to be known is that in a $\mathbf{B}$ field the $\boldsymbol{\mu}$ moment has a potential energy that depends on the angle θ. According to convention, the potential energy E_μ^{pot} of a magnetic moment $\boldsymbol{\mu}$ in a magnetic field $\mathbf{B}$ is defined as the work W done by the torque $\mathbf{T}$ on $\boldsymbol{\mu}$ when it causes the reference angle $\theta = \pi/2$ to change to an arbitrary value θ':

$$E_\mu^{\text{pot}} = W = \int_{\pi/2}^{\theta} T d\theta' = \int_{\pi/2}^{\theta} \mu B \sin\theta' d\theta' = -\mu B \cos\theta = -\boldsymbol{\mu}\cdot\mathbf{B} \tag{2.3}$$

This means that the energy of the magnetic moment is at a minimum, $E_\mu^{\text{pot}} = -\mu B$, when $\boldsymbol{\mu}$ is aligned parallel with $\mathbf{B}$ ($\theta = 0$), it is zero when $\boldsymbol{\mu}$ and $\mathbf{B}$ are perpendicular ($\theta = \pi/2$), and it is at a maximum, $E_\mu^{\text{pot}} = \mu B$, when $\boldsymbol{\mu}$ is antiparallel with $\mathbf{B}$ ($\theta = \pi$). The negative energy value associated with the stable equilibrium position of $\theta = 0$ may first seem puzzling because intuition would dictate that when the moment lines up with the field, the potential energy should be zero. The answer to this problem is that potential energy is defined as the energy difference between the energy of an object in a given position and its energy at a reference position; it is the work done by a so-called conservative force (whose work done when moving an object does not depend on the path) against a reference position. As noted above, with regard to the magnetic potential energy this zero-energy reference point has been conventionally defined as the position when the magnetic moment is perpendicular to $\mathbf{B}$. Conceptually, when starting from this position, an increase in the angle θ requires work, that is, an increase in energy, while by "letting go" of the magnetic moment, $\mathbf{B}$ will do work through the torque (2.1) on the moment to align it onto itself, which means a negative potential energy.

According to the fundamental laws of classical mechanics, when a force acts on a spinning object such that it wants to change the spatial orientation of the object's axis of rotation (i.e., the direction of the $\mathbf{P}$ vector), then the axis (i.e., $\mathbf{P}$) will move not in the direction of the force, but in the direction of the torque generated by the force. In the case of the magnetic moment $\boldsymbol{\mu}$ with a spin $\mathbf{P}$ this can be described quantitatively from (2.1) as

$$\frac{d\mathbf{P}}{dt} = \mathbf{T} = \boldsymbol{\mu} \times \mathbf{B}. \tag{2.4}$$

(Note that Eq. (2.4) is valid only for a *gyro*-magnetic moment.) When (2.4) is combined with (2.2), we obtain the following well-known equation of motion for the spinning magnetic dipole:

$$\frac{d\boldsymbol{\mu}}{dt} = \gamma[\boldsymbol{\mu} \times \mathbf{B}]. \tag{2.5}$$

Equation (2.5) describes the uniform precession of $\boldsymbol{\mu}$ about the $\mathbf{B}$ vector on the surface of a circular cone with semi-angle θ (we speak of a precessing vector if the tip rotates about an axis when the tail is fixed). Because θ is a constant of the motion, the energy E_μ^{pot} specified by

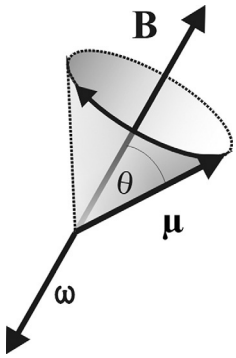

FIGURE 2.1 Larmor precession.

Eq. (2.3) also remains constant (Fig. 2.1). This motion is the famous *Larmor precession* whose direction and angular frequency are given, as can be derived from (2.5), by the expression

$$\boldsymbol{\omega} = -\gamma \mathbf{B}\,(\text{i.e.}, \omega = 2\pi\nu = \gamma B). \tag{2.6}$$

In liquid-state NMR spectroscopy, our initial physical condition is always that we place the sample (i.e., our spin ensemble as specified above) in a strong static homogeneous magnetic field which is universally denoted by the vector $\mathbf{B}_0$. From (2.1) we see that in the $\mathbf{B}_0$ field any given spin will experience a torque $\mathbf{T} = \boldsymbol{\mu} \times \mathbf{B}_0$ and thus (2.5) will become

$$\frac{d\boldsymbol{\mu}}{dt} = \gamma[\boldsymbol{\mu} \times \mathbf{B}_0] \tag{2.7}$$

so that $\boldsymbol{\mu}$ will precess about $\mathbf{B}_0$ with a Larmor angular frequency

$$\boldsymbol{\omega}_0 = -\gamma \mathbf{B}_0 \tag{2.8}$$

by maintaining a constant θ angle and thereby a constant energy E_μ^{pot}. This situation is commonly portrayed within a right-handed 3D Cartesian coordinate system (x,y,z), specified such that the $+x$, $+y$, and $+z$ axes point in the direction of the unitary vectors $\mathbf{e}_x$, $\mathbf{e}_y$, and $\mathbf{e}_z$, respectively; the right-handedness of the system is defined through the condition $\mathbf{e}_x \times \mathbf{e}_y = \mathbf{e}_z$. In this system, $\mathbf{B}_0$ is chosen to point in the $+z$ ("longitudinal") direction as shown in Fig. 2.2.

NMR spectroscopy essentially deals with the phenomenon of how this Larmor-precessing spin, or an ensemble of such spins, can be brought to "resonate" if we subject it to a second, harmonically oscillating $\mathbf{B}_1$ magnetic field which is much weaker than $\mathbf{B}_0$ (i.e., $B_1 \ll B_0$) and whose driving frequency ω_{D} is near the Larmor frequency ω_0. The spin thus experiences an effective field

$$\mathbf{B}_{\text{eff}} = \mathbf{B}_0 + \mathbf{B}_1. \tag{2.9}$$

The fluctuating $\mathbf{B}_1$ field is generated by an RF coil surrounding the sample such that the driving field can be *regarded* as a $\mathbf{B}_1$ vector which rotates in the (x,y) plane (the "transversal" plane) in the same direction as the Larmor precession (i.e., $\boldsymbol{\omega}_0$ and $\boldsymbol{\omega}_{\text{D}}$ point in the same

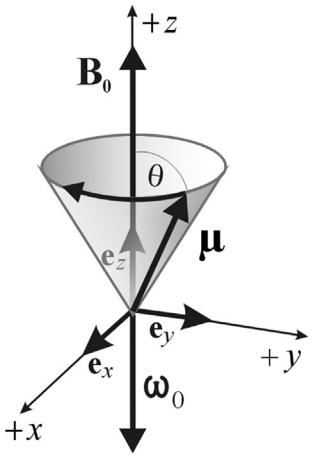

FIGURE 2.2 Larmor precession in a $\mathbf{B}_0$ static field in a Cartesian system.

direction) as shown in Fig. 2.3 (this statement is subtle, and the word "regarded" is intentionally italicized; I will return to this point in Chapter 5). The driving field will exert a second torque $\mathbf{T} = \boldsymbol{\mu} \times \mathbf{B}_1$ on the magnetic moment, and so the equation of motion (2.5) will become

$$\frac{d\boldsymbol{\mu}}{dt} = \gamma[\boldsymbol{\mu} \times (\mathbf{B}_0 + \mathbf{B}_1)] = \gamma[\boldsymbol{\mu} \times \mathbf{B}_{\text{eff}}]. \tag{2.10}$$

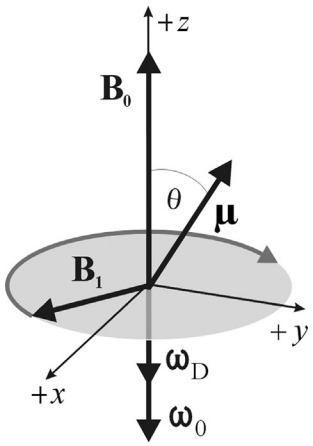

FIGURE 2.3 The magnetic moment in a $\mathbf{B}_0$ static field and a $\mathbf{B}_1$ driving field rotating in the (x,y) plane (the depicted vector lengths are illustrative only, e.g., in reality $B_1 \ll B_0$).

In order to understand how the rotating $\mathbf{B}_1$ field induces resonance in the $\boldsymbol{\mu}$ magnetic moment, it may be useful (but not necessary) to draw, as a first approximation, an analogy with a linear harmonic oscillator, such as a spring with a small weight hung on it, which is subjected to a sinusoid driving force, such as we jerk it up and down as we hold the upper end of the spring. Simple resonance theory states that this linear oscillator (resonator) has a natural frequency (eigen frequency) ω_0, and if we suddenly act upon it with a sinusoidal driving force oscillating with frequency ω_D in the same direction as the oscillator, then after a short time, during which it adapts to the new condition, the driven oscillator will no longer oscillate with its eigen frequency, but will be forced to oscillate at the frequency of the driving force (i.e., the oscillation of the resonator will not be independent of the driving frequency). The amplitude of this driven oscillation will be small if $\omega_D \ll \omega_0$ or $\omega_D \gg \omega_0$, but it will be maximal when $\omega_0 = \omega_D$, which is the resonance condition. Similarly, in magnetic resonance $\boldsymbol{\mu}$ can be thought of as a resonator whose Larmor frequency ω_0 is the natural frequency, and the rotating $\mathbf{B}_1$ field acts as the driving force with angular frequency ω_D. The amplitude of the motion of $\boldsymbol{\mu}$ is taken to be the magnitude of its projection onto the (x,y) plane. Because in magnetic resonance we are dealing with rotating rather than linearly oscillating entities, the response of the system to the driving force will be more complex. (The analogy with the linear oscillator should not be over-interpreted: it is merely used here as a familiar everyday example that is easy to relate to, and which shows that a driven oscillator no longer oscillates with the free oscillator's eigenfrequency. Nevertheless, we should expect that the physics behind the linear and the precessing driven resonators should be analogous to the extent that in both cases the resonator will take on the driving frequency.)

The way the "driven" $\boldsymbol{\mu}$ oscillator actually behaves in a $\mathbf{B}_{\text{eff}}$ field is rather fascinating. Because it is neither intuitively, nor mathematically easy to infer this motion in a moving $\mathbf{B}_{\text{eff}}$ field, a trick almost universally employed to overcome this difficulty is to convert Eq. (2.10) into a rotating Cartesian frame[6] designed so as to make $\mathbf{B}_{\text{eff}}$ static. The procedure rests on the following simple mathematical consideration. Besides our (x,y,z) Cartesian system which is fixed in the laboratory, we take a second Cartesian frame (x',y',z) whose origin is coincident with the laboratory frame but which rotates about the z axis with angular velocity $\boldsymbol{\omega}$ with respect to (x,y,z). If we now consider a vector $\mathbf{v}$ which is stationary in the laboratory frame (x,y,z), that is, $d\mathbf{v}/dt = 0$, then an observer positioned within the rotating frame (x',y',z) will perceive $\mathbf{v}$ as rotating with angular velocity $-\boldsymbol{\omega}$, that is, from that perspective $(d\mathbf{v}/dt)_{\text{rot}} = -\boldsymbol{\omega} \times \mathbf{v}$. If $\mathbf{v}$ is a function of time in (x,y,z), that is, $d\mathbf{v}/dt \neq 0$, then an observer in (x',y',z) will perceive $\mathbf{v}$ as rotating according to $-\boldsymbol{\omega} \times \mathbf{v}$ as well as changing according to its motion $d\mathbf{v}/dt$ within the (x,y,z) frame. Thus, any $\mathbf{v}$ vector in the stationary frame (x,y,z) can be transformed into the rotating frame (x',y',z) by the equation

$$\left(\frac{d\mathbf{v}}{dt}\right)_{\text{rot}} = \frac{d\mathbf{v}}{dt} - \boldsymbol{\omega} \times \mathbf{v}. \tag{2.11}$$

The particular rotating frame used in NMR is a frame (x',y',z) which rotates about the z axis in synch with the driving $\mathbf{B}_1$ field, that is, with angular frequency $\boldsymbol{\omega}_D$ so that $\mathbf{B}_1$ appears static for the rotating-frame observer. By default, the $\mathbf{B}_1$ vector is conventionally drawn along the x' axis (although it is by no means restricted to that direction). Applying Eq. (2.11), the transformation equation for the $\boldsymbol{\mu}$ vector becomes

$$\left(\frac{d\boldsymbol{\mu}}{dt}\right)_{\text{rot}} = \frac{d\boldsymbol{\mu}}{dt} - \boldsymbol{\omega}_{\text{D}} \times \boldsymbol{\mu} = \frac{d\boldsymbol{\mu}}{dt} + \boldsymbol{\mu} \times \boldsymbol{\omega}_{\text{D}}. \tag{2.12}$$

Using Eq. (2.12), Eq. (2.10) converts into the rotating frame as

$$\left(\frac{d\boldsymbol{\mu}}{dt}\right)_{\text{rot}} = \gamma\left[\boldsymbol{\mu} \times \left(\mathbf{B}_0 + \mathbf{B}_1 + \frac{\boldsymbol{\omega}_{\text{D}}}{\gamma}\right)\right] = \gamma\left[\boldsymbol{\mu} \times \mathbf{B}_{\text{eff}}^{\text{rot}}\right]. \tag{2.13}$$

Note the term $\boldsymbol{\omega}_{\text{D}}/\gamma$, which appears in Eq. (2.13) as a consequence of the factor $\boldsymbol{\mu} \times \boldsymbol{\omega}_{\text{D}}$ in Eq. (2.12), and which formally opposes $\mathbf{B}_0$, so that we have $|\mathbf{B}_0 + \boldsymbol{\omega}_{\text{D}}/\gamma| = B_0 - \omega_{\text{D}}/\gamma$. As a result, the effective field $\mathbf{B}_{\text{eff}}^{\text{rot}}$ "felt" by $\boldsymbol{\mu}$ in the rotating frame becomes

$$\mathbf{B}_{\text{eff}}^{\text{rot}} = \mathbf{B}_0 + \mathbf{B}_1 + \frac{\boldsymbol{\omega}_{\text{D}}}{\gamma} \tag{2.14}$$

as shown in Fig. 2.4.

The concept of resonance can now be interpreted in a rather simple and intuitively convenient way. Since $\mathbf{B}_{\text{eff}}^{\text{rot}}$ is static in the rotating frame, according to the generic rules (2.5) and (2.6), Eq. (2.13) tells us that $\boldsymbol{\mu}$ precesses about $\mathbf{B}_{\text{eff}}^{\text{rot}}$ with frequency

$$\boldsymbol{\omega}_{\text{eff}}^{\text{rot}} = -\gamma \mathbf{B}_{\text{eff}}^{\text{rot}}. \tag{2.15}$$

If we imagine varying the frequency ω_{D} of the $\mathbf{B}_1(t)$ field, then, according to Eq. (2.14), in the rotating frame the magnitude and direction of $\mathbf{B}_{\text{eff}}^{\text{rot}}$ will also change. When the term $\boldsymbol{\omega}_{\text{D}}/\gamma$ cancels $\mathbf{B}_0$ exactly in (2.14), that is, when $B_0 = \omega_{\text{D}}/\gamma$, we have $\mathbf{B}_{\text{eff}}^{\text{rot}} = \mathbf{B}_1$. In this case, the net field experienced by $\boldsymbol{\mu}$ in the rotating frame is only $\mathbf{B}_1$, so $\boldsymbol{\mu}$ conducts Larmor precession about this field with frequency

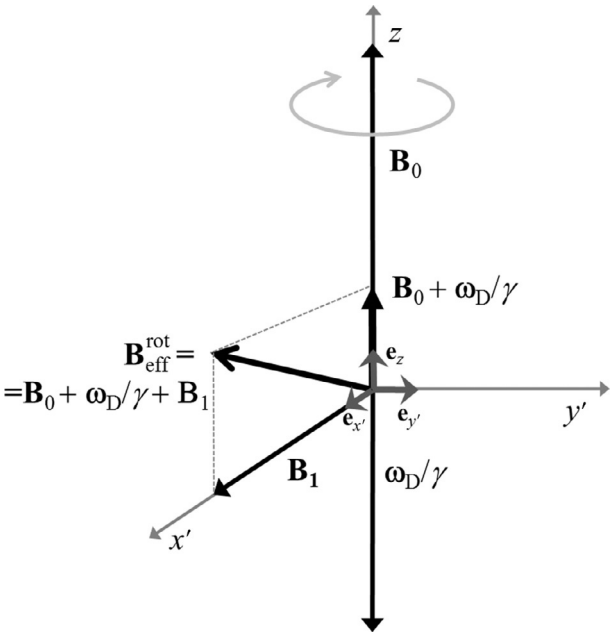

FIGURE 2.4 The rotating frame of reference.

$$\boldsymbol{\omega}_1 = -\gamma \mathbf{B}_1. \tag{2.16}$$

From Fig. 2.4, it can be readily seen that under this condition the precessing $\boldsymbol{\mu}$ vector will give the largest maximum projection onto the (x',y') plane, which is why it is called the *resonance* condition. Note that the resonance condition $B_0 = \omega_D/\gamma$ means (cf. Eq. 2.8) that

$$\boldsymbol{\omega}_D = -\gamma \mathbf{B}_0 = \boldsymbol{\omega}_0. \tag{2.17}$$

If we now want to envisage the motion of $\boldsymbol{\mu}$ in the laboratory frame, all we have to do is take this rotating-frame result and allow it to rotate about the z axis with frequency $\boldsymbol{\omega}_D$, thus we obtain a motion according to which $\boldsymbol{\mu}$ precesses about an axis defined by $\mathbf{B}_{\text{eff}}^{\text{rot}}$, and this axis itself precesses with frequency $\boldsymbol{\omega}_D$ about the z axis.

The above explanation, involving the rotating frame, is an elegant and useful description of magnetic resonance, and one may indeed claim to have gained from it a good and pictorially accessible understanding of the essence of the resonance condition. Let us, however, look at this portrayal of magnetic resonance by introducing a touch of "AA-eye," particularly with regard to the nature of human understanding (Pillar 6) and the way we can confuse mathematical descriptions with physical understanding (Trap #11).

We arrived at the rotating-frame description by a purely mathematical transformation using Eq. (2.11), and then we started explaining whatever happens in the rotating frame physically, that is, in a "mixed-mind-state" (cf. Trap #11). However, the rotating frame can be a tricky affair: it apparently simplifies things, but it is also a non-inertial frame, and non-inertial frames are famous for their need to introduce fictitious forces to explain observed motions (just think of the well-known Coriolis force or centrifugal force which are both fictitious entities that exist only in a rotating frame of observation). Events in non-inertial frames are often not easily translated into a physical understanding pertaining to the inertial physical world that we live in, that with which we are familiar with, and that from which we draw our experiential knowledge of Nature. In this respect, I want to bring up the following issue about the rotating frame as a potential source of illusive understanding.

Consider the $\boldsymbol{\omega}_D/\gamma$ factor that appears in the rotating-frame Eqs. (2.13) or (2.14). As we have seen, this term is central to our physical rotating-frame understanding of magnetic resonance, but in fact it transpires from a mathematical necessity dictated by Eq. (2.11). We normally step over this problem (if it is perceived as a problem at all) by noting that the term $\boldsymbol{\omega}_D/\gamma$ formally has identical features to a real magnetic field, so we start calling it a "virtual field" or a "fictitious field," usually without mulling too much over what exactly that means. Even if we do, we can readily convince ourselves that $\boldsymbol{\omega}_D/\gamma$ indeed acts as a field. After all, the fact that $\boldsymbol{\omega}_D/\gamma$ emerges as a mathematical consequence when going into the rotating frame must surely justify its presence there also as a physical necessity (note the slight emotycal overtone in this argument). Moreover, since we are in a noninertial frame, the presence of a fictitious field should not be too surprising. Indeed, if we forget about the $\mathbf{B}_1$ field for a moment and think about laboratory-frame Larmor precession in the $\mathbf{B}_0$ field as shown in Fig. 2.2 and expressed by Eq. (2.8), and imagine that we observe this motion from a frame rotating exactly with the Larmor frequency $\boldsymbol{\omega}_D = \boldsymbol{\omega}_0$, then in this frame the magnetic moment is static, therefore Larmor precession seizes. Clearly, this is only possible if there is no net $\boldsymbol{\mu} \times \mathbf{B}$ torque acting upon the magnetic moment, that is, there must be "something" compensating the $\mathbf{B}_0$ field so that the net $\mathbf{B}$ field experienced by $\boldsymbol{\mu}$ is zero. The term $\boldsymbol{\omega}_D/\gamma = \boldsymbol{\omega}_0/\gamma$ does exactly this

"job," which seems to validate the idea that $\boldsymbol{\omega}_D/\gamma$ can be treated as a field. Furthermore, the concept of $\boldsymbol{\mu}$ rotating about the effective field (2.14) is conveniently consistent with its equation of motion according to (2.5). In all, the whole scenario serves our intuition well, especially if one is not aware of, or bothered by, thinking about it in mixed-mind-state mode. However, if we choose to get sharply sensitive about the difference between mathematical and physical understanding according to Pillar 6, then we should be honest about the fact that what we have really done is we have welded a piece of mathematical truth into our physical understanding of magnetic resonance, attributing to $\boldsymbol{\omega}_D/\gamma$ a *post hoc* physical meaning, essentially claiming that $\boldsymbol{\omega}_D/\gamma$ is physically there because it is mathematically there. Sure enough, $\boldsymbol{\omega}_D/\gamma$ can be legitimately proclaimed to be a fictitious non-inertial-frame entity, but does this mean that we have truly understood its deeper physical meaning beyond just making the more or less "sterile" statement that it is a fictitious field? In essence, we have achieved simplicity at the expense of introducing a fictitious field which, for many people, somehow remains vaguely understood.

When we have inferred the laboratory-frame motion of $\boldsymbol{\mu}$ not directly in the laboratory frame, but by first making a digression into the rotating frame, then we have essentially injected into our physical understanding this piece of mathematically conjured ingredient. Most NMR-literate persons, if asked about the physical meaning of the $\boldsymbol{\omega}_D/\gamma$ term, will start recounting the above rotating-frame argument. However, if challenged to explain the magnetic resonance phenomenon directly in the laboratory frame where there are no fictitious elements coming up as a result of mathematical considerations, people often become puzzled. It may be worthwhile to examine this situation through the following considerations.

As was discussed in connection with Fig. 2.4, in the rotating frame our apperception of resonance transpires from the concept that the angle $\mathbf{B}_{\text{eff}}^{\text{rot}} \measuredangle \mathbf{e}_z$ between $\mathbf{B}_{\text{eff}}^{\text{rot}}$ and $\mathbf{e}_z$ increases from almost zero to 90° as we increase the driving frequency from $\omega_D \ll \omega_0$ to $\omega_D = \omega_0$. As a result, at resonance $\boldsymbol{\mu}$ precesses exclusively about $\mathbf{B}_1$ as being the only field that it effectively experiences. The axis of this "resonant" precession is perpendicular to the original axis of Larmor precession about the $\mathbf{B}_0$ field, which allows $\boldsymbol{\mu}$ to attain its maximal amplitude of motion in the (x,y) plane. However, if we try to envisage resonance directly in the laboratory frame, our intuitive understanding based on the rotating-frame description might easily lead to an apparently puzzling predicament according to the following reasoning. Imagine, in the laboratory frame, the initial situation in which the $\boldsymbol{\mu}$ vector is precessing about the $\mathbf{B}_0$ field with a small angle θ. Because in the laboratory frame there is no $\boldsymbol{\omega}_D/\gamma$ term, upon turning on the rotating $\mathbf{B}_1$ field the effective field felt by $\boldsymbol{\mu}$ will be $\mathbf{B}_{\text{eff}} = \mathbf{B}_0 + \mathbf{B}_1$ according to (2.9), and this $\mathbf{B}_{\text{eff}}$ vector will be precessing about the z axis with constant frequency ω_D and with a constant angle $\mathbf{B}_{\text{eff}} \measuredangle \mathbf{e}_z$ between $\mathbf{B}_{\text{eff}}$ and $\mathbf{e}_z$. Note that because $B_0 \gg B_1$, the $\mathbf{B}_{\text{eff}}$ vector is only very slightly tilted away from the z axis, that is, $\mathbf{B}_{\text{eff}} \measuredangle \mathbf{e}_z \approx 0$. By analogy with Eq. (2.5) whose solution is Eq. (2.6), one may expect that the solution of (2.10) will also be a uniform Larmor precession of $\boldsymbol{\mu}$ about this moving $\mathbf{B}_{\text{eff}}$ field, with frequency $\boldsymbol{\omega}_{\text{eff}} = -\gamma \mathbf{B}_{\text{eff}}$. But because the effective field felt by $\boldsymbol{\mu}$ now has a constant angle $\mathbf{B}_{\text{eff}} \measuredangle \mathbf{e}_z$ for all values of ω_D (as opposed to the rotating frame in which the effective field felt by $\boldsymbol{\mu}$ changes the angle $\mathbf{B}_{\text{eff}}^{\text{rot}} \measuredangle \mathbf{e}_z$ as a function of ω_D), the expected Larmor precession of $\boldsymbol{\mu}$ about $\mathbf{B}_{\text{eff}}$, which is almost parallel with z, cannot cause such a tilting away of $\boldsymbol{\mu}$ from the z axis at the resonance condition $\omega_D = \omega_0$ as what we have inferred from the rotating-frame considerations. Moreover, note that the result of this reasoning is different from that obtained when we first went into the rotating frame and then

transformed the rotating-frame result (Fig. 2.4) into the laboratory frame by allowing the former to rotate about the z axis with frequency $\boldsymbol{\omega}_D$. According to that reasoning, in the laboratory frame $\boldsymbol{\mu}$ will also precesses about the axis of $\mathbf{B}_{\text{eff}}^{\text{rot}}$ even though $\mathbf{B}_{\text{eff}}^{\text{rot}}$ should now not "exist" in the absence of the term $\boldsymbol{\omega}_D/\gamma$. This means that the intuitive idea that in the laboratory frame $\boldsymbol{\mu}$ should precess about $\mathbf{B}_{\text{eff}}$ must be wrong. It is therefore interesting to see if we can make some physical sense, *without* using the rotating frame, of why, in the laboratory frame, $\boldsymbol{\mu}$ precesses about an axis that is tilted *downward* of $\mathbf{B}_{\text{eff}}$, instead of precessing about $\mathbf{B}_{\text{eff}}$ itself. Note, as a starting point, that because the resonance condition $\omega_D = \omega_0$ was arrived at by equating ω_D/γ with B_0 in the rotating frame, and this resonance condition must equally be valid in the laboratory frame, we can expect that $\boldsymbol{\omega}_D/\gamma$ must somehow appear as a physical entity also in the laboratory frame (and not just as an abstraction coming from Eq. 2.12). One way to render a physically more palpable meaning to $\boldsymbol{\omega}_D/\gamma$ is as follows.

Imagine, as a thought experiment, that the $\mathbf{B}_1$ field is initially static in the laboratory frame and points in the direction of the $+y$ axis, so we have a static effective field $\mathbf{B}_{\text{eff}}$ in the (z,y) plane, and let our starting condition be such that $\boldsymbol{\mu}$ happens to point along $\mathbf{B}_{\text{eff}}$. Now let us allow the $\mathbf{B}_1$ field vector to *suddenly* start rotating with frequency $\boldsymbol{\omega}_D$ about the z axis, so $\mathbf{B}_{\text{eff}}$ also starts precessing. If the $\mathbf{B}_1$ vector has moved by a small angle $\delta\vartheta$ away from the $+y$ axis in a short time δt, then $\mathbf{B}_{\text{eff}}$ will have also moved away by an angle $\delta\vartheta$ from both the $+y$ axis and from $\boldsymbol{\mu}$ (note that, as opposed to the case when $\mathbf{B}_{\text{eff}}$ changes so slowly that $\omega_D \ll \gamma B_{\text{eff}}$, which is called the adiabatic condition, $\boldsymbol{\mu}$ will not stay "glued" to $\mathbf{B}_{\text{eff}}$ if we impart a sudden rotation upon the latter). This situation creates a torque $\boldsymbol{\mu} \times \mathbf{B}_{\text{eff}}$ which is in the (z,y) plane, and which will tilt $\boldsymbol{\mu}$ by a small angle $\delta\epsilon$, in a time δt, toward the $+y$ axis. During the next small δt time interval, $\mathbf{B}_{\text{eff}}$ will again move by a further $\delta\vartheta$ angle away from the $+y$ axis as well as from $\boldsymbol{\mu}$, thus increasing slightly the torque $\boldsymbol{\mu} \times \mathbf{B}_{\text{eff}}$. Also, because $\boldsymbol{\mu}$ has moved downward toward the $+y$ axis in the previous step, the present torque $\boldsymbol{\mu} \times \mathbf{B}_{\text{eff}}$ is no longer in the (z,y) plane, but is now slightly skewed toward the $+x$ axis, therefore it tilts $\boldsymbol{\mu}$ further down by slightly moving it also toward the $+x$ axis. In all, $\boldsymbol{\mu}$ lags behind $\mathbf{B}_{\text{eff}}$ and follows it along an arc according to the way the torque $\boldsymbol{\mu} \times \mathbf{B}_{\text{eff}}$ changes during the process. If one follows this train of thought, with a bit of imagination it is easy to see that the tip of $\boldsymbol{\mu} \times \mathbf{B}_{\text{eff}}$ must trace a circle as it moves under the influence of the changing $\boldsymbol{\mu} \times \mathbf{B}_{\text{eff}}$ torque, eventually catching up with $\mathbf{B}_{\text{eff}}$, whereby the process starts again. This circle will be the base of a cone traced by $\boldsymbol{\mu}$ as it follows the precessing $\mathbf{B}_{\text{eff}}$ field. We may think of this process as $\boldsymbol{\mu}$ attempting to precess about $\mathbf{B}_{\text{eff}}$ with frequency $-\gamma\mathbf{B}_{\text{eff}}$, but $\mathbf{B}_{\text{eff}}$ keeps "running away" from $\boldsymbol{\mu}$ with frequency $\boldsymbol{\omega}_D$. The way $\boldsymbol{\mu}$ can catch up with $\mathbf{B}_{\text{eff}}$ is by lagging behind until the torque $\boldsymbol{\mu} \times \mathbf{B}_{\text{eff}}$ becomes large enough and of the proper direction so that it can drive $\boldsymbol{\mu}$ back onto $\mathbf{B}_{\text{eff}}$ again. The closer the frequency ω_D is to the frequency γB_{eff} with which $\boldsymbol{\mu}$ attempts to precesses about the net field $\mathbf{B}_{\text{eff}}$ that it "feels," the larger the angle $\delta\epsilon$ traveled by $\boldsymbol{\mu}$ while $\mathbf{B}_{\text{eff}}$ travels the angle $\delta\vartheta$ in a time δt, therefore the larger the θ_b angle of the cone traced by $\boldsymbol{\mu}$ will be. Thus, $\boldsymbol{\mu}$ does not conduct a simple Larmor precession about the moving $\mathbf{B}_{\text{eff}}$ field as one might intuitively expect from drawing a hasty analogy with Fig. 2.1, but exhibit an intricate motion involving Larmor precession about a moving axis which is tilted *away* from $\mathbf{B}_{\text{eff}}$.

The above motion can be better understood and visualized by applying the rules of rigid-body dynamics, as was originally pointed out by Corio.[7] The situation is first illustrated for the off-resonance condition where $\omega_D < \omega_0$ in Fig. 2.5.

In order to understand the essence of Fig. 2.5, we need to lean on a theorem by Euler which states that any displacement of a 3D rigid body with one point fixed in space (this point may

or may not be in the body itself) can in any instant be described as a *single* rotation about some *single* axis, called the *instantaneous axis of rotation*, with the points of the body falling on this axis being momentarily at rest. In fact, it can be shown from Euler's theorem that the most general motion of any point of a rigid body with one point fixed consists of the *rolling* without slipping of a cone fixed in the body (called the *body cone*) upon a cone fixed in space (called the *space cone*) such that the vertices of the two cones are at the fixed point. (In general, neither of these cones is necessarily circular, but when applying these concepts to the motion of $\boldsymbol{\mu}$, the cones are of course circular.) According to this description, a point on the body cone precesses about the *central axis of rotation of the body cone*. Similarly, the instantaneous axis of rotation itself precesses about the *central axis of rotation of the space cone*.

If we adopt the above principles to the motion of $\boldsymbol{\mu}$ in the laboratory frame as shown in Fig. 2.5, we see that at any given instant the space cone and the body cone are tangent along the instantaneous axis of rotation R^i which coincides with the net effective field vector $\mathbf{B}_{\text{eff}} = \mathbf{B}_0 + \mathbf{B}_1$ and which precesses with frequency $\boldsymbol{\omega}_D$ about the central axis of rotation of the space cone, which of course is the z axis that is coincident with $\mathbf{B}_0$. The central axis of rotation of the body cone is the Q axis about which $\boldsymbol{\mu}$ precesses with frequency $\boldsymbol{\omega}_Q$. The plane through the R^i and z axes passes through the Q axis, and this plane turns round the z axis also with angular velocity $\boldsymbol{\omega}_D$. Thus, the axis Q rotates in

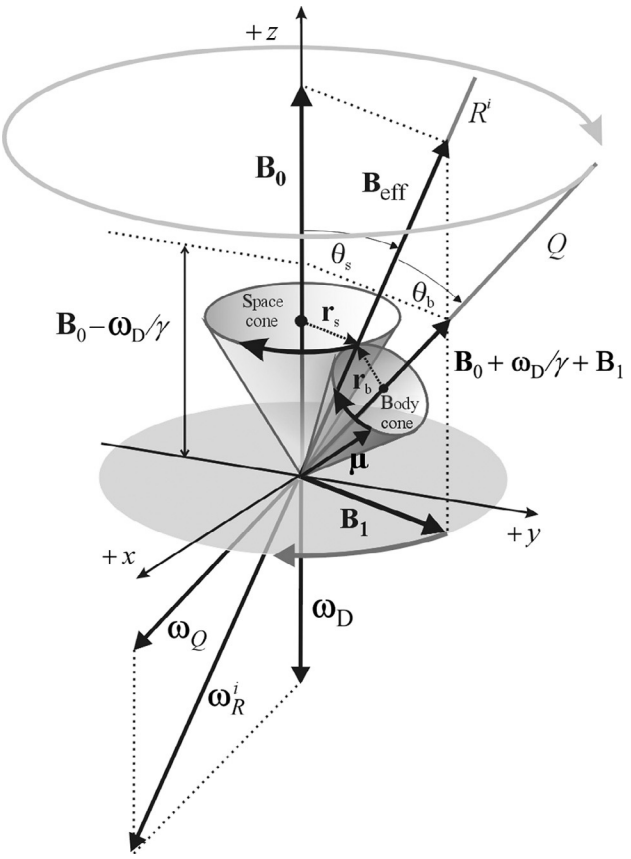

FIGURE 2.5 Conceptual illustration of the motion of an isolated magnetic moment $\boldsymbol{\mu}$ in a $\mathbf{B}_0$ static field and a $\mathbf{B}_1$ driving field rotating in the (x,y) plane for the off-resonance case when $\omega_D < \omega_0$. Using the ideas of rigid-body dynamics, the magnetic moment precesses about the central axis of rotation Q, forming a *body cone* which rolls without slipping on the *space cone* along the instantaneous axis of rotation R^i. For illustrative purposes, the length of $\mathbf{B}_1$ is greatly exaggerated. In reality, $B_1 \ll B_0$, and therefore θ_s is very small.

the (x,y) plane in synch with the rotating $\mathbf{B}_1$ field in analogy with the way the driven harmonic linear resonator takes up the frequency of the driving force. In this motion the body cone rolls without slipping on the space cone. The body cone and space cone are both circular and have semi-angles θ_b and θ_s, respectively. Note that in reality $\theta_s \approx 0$ because $B_1 \ll B_0$, therefore R^i almost coincides with the z axis. While the semi-angle θ_s of the space cone is constant, θ_b depends on the difference between ω_D and ω_0.

In order for the rolling-without-slipping condition to hold, ω_D must clearly bear a constant ratio to ω_Q. This condition is satisfied if the radius vectors $\mathbf{r}_b$ and $\mathbf{r}_s$ rotate about the Q and the z axes, respectively, according to the condition $d\mathbf{r}_b/dt = d\mathbf{r}_s/dt$. From this, the rolling-without-slipping condition holds if

$$\frac{dr_b}{dt} = r_b\omega_Q \equiv \frac{dr_s}{dt} = r_s\omega_D, \text{ (i.e., if } \omega_Q/\omega_D = r_s/r_b). \tag{2.18}$$

Another basic theorem of rigid-body mechanics ensuing from the above considerations states that at any point in time the instantaneous angular frequency $\boldsymbol{\omega}_R^i$ with which $\boldsymbol{\mu}$ precesses about the instantaneous axis of rotation R^i, and therefore also the instantaneous *direction* of R^i, can be simply obtained by adding $\boldsymbol{\omega}_D$ and $\boldsymbol{\omega}_Q$, that is,

$$\boldsymbol{\omega}_R^i = \boldsymbol{\omega}_D + \boldsymbol{\omega}_Q. \tag{2.19}$$

We know of course that $\boldsymbol{\omega}_R^i = \boldsymbol{\omega}_{\text{eff}}^i = -\gamma\mathbf{B}_{\text{eff}} = -\gamma\mathbf{B}_0 - \gamma\mathbf{B}_1$, so from Eq. (2.19) we have

$$\boldsymbol{\omega}_Q = -\gamma\mathbf{B}_0 - \gamma\mathbf{B}_1 - \boldsymbol{\omega}_D = -\gamma\left(\mathbf{B}_0 + \mathbf{B}_1 + \frac{\boldsymbol{\omega}_D}{\gamma}\right). \tag{2.20}$$

We see from Eq. (2.20) that the term $\boldsymbol{\omega}_D/\gamma$ has appeared again as a factor that plays an important role in determining the axis about which $\boldsymbol{\mu}$ conducts Larmor precession on the surface of the body cone, and from Eq. (2.14) it is evident that this axis corresponds directly with the direction of $\mathbf{B}_{\text{eff}}^{\text{rot}}$ that we are already familiar with from the rotating frame. However, the laboratory-frame result (2.20) immediately renders a more tangible physical meaning to $\boldsymbol{\omega}_D/\gamma$ than the fictitious entity that appeared in the rotating frame. These considerations show that the value of θ_s is uniquely determined by the B_0-to-B_1 ratio, while the value of θ_b is uniquely determined by the B_0-to-B_1 ratio *as well as* the angular frequency ω_D with which the $\mathbf{B}_1$ field rotates. In a way we may think of $\boldsymbol{\omega}_D/\gamma$ as a factor which ensures that at any given instant the axis of the body cone is tilted away from the instantaneous axis R^i to the exact degree so that $\boldsymbol{\mu}$ can roll without slipping on the space cone while its axis of Larmor precession Q moves in synch with the precession of the $\mathbf{B}_{\text{eff}}$ field about the z axis.

The situation is also illustrated pictorially for the resonance condition in Fig. 2.6. This figure is instructive from the particular point of view that at resonance the rolling-without-slipping condition expressed in Eq. (2.18) is directly seen to be $\omega_Q/\omega_D = r_s/r_b = B_0/B_1$, in line with the fact that in this case the Q axis coincides with the $\mathbf{B}_1$ field and thus we simply have $\boldsymbol{\omega}_Q = -\gamma\mathbf{B}_1$ (cf. Eq. 2.20). Since by definition $\boldsymbol{\omega}_R^i = -(\gamma\mathbf{B}_0 + \gamma\mathbf{B}_1)$, from Eq. (2.19) we thus obtain $\boldsymbol{\omega}_R^i = -(\gamma\mathbf{B}_0 + \gamma\mathbf{B}_1) = \boldsymbol{\omega}_D - \gamma\mathbf{B}_1$, from which $\omega_D = \gamma B_0 = \omega_0$, which is just the resonance condition (2.17).

The off-resonance condition corresponding to $\omega_D > \omega_0$ is illustrated in Fig. 2.7, which should give an added level of understanding to the rigid-body dynamical representation

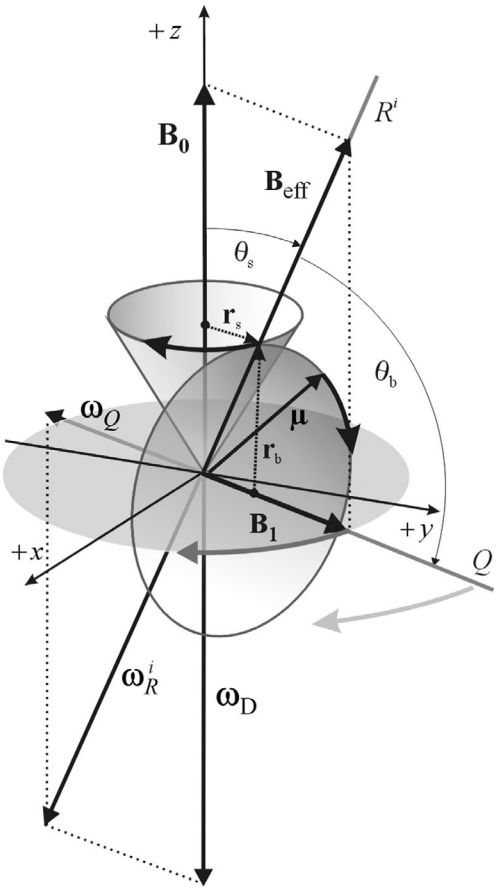

FIGURE 2.6 Conceptual illustration of the motion of an isolated magnetic moment $\boldsymbol{\mu}$ in the laboratory frame in a $\mathbf{B}_0$ static field and a $\mathbf{B}_1$ driving field rotating in the (x,y) plane for the on-resonance case when $\omega_D = \omega_0$. In reality, $B_1 \ll B_0$, and therefore $\theta_s \approx 0$. This is a case of a convex body cone rolling on the outside of a convex space cone.

of magnetic resonance. Note, in that respect, that in Figs. 2.5 and 2.6 the body cone and the space cone are convex, with the body cone rolling on the exterior of the space cone. However, for the off-resonance condition $\omega_D > \omega_0$ the body cone is concave, rolling with its interior on the exterior of the convex space cone. Of particular interest here is the fact that in this case the overall rotation of the body cone is opposite to the sense of precession of the Q axis. This motion is known as *retrograde* rotation, as opposed to the "regular" rotation seen in Figs. 2.5 and 2.6. Really "seeing" this motion may tax one's imagination, but it may be helpful in that regard to make the mental transition from the convex-convex to the convex-concave scenario by imagining that we "flip" the convex body cone of Fig. 2.6 into a concave cone as shown in Fig. 2.7 while maintaining the sense of rotation of $\boldsymbol{\mu}$.

The above description of NMR in the static frame should be treated in its proper context. It is of course much easier to envisage the motion of the magnetic moment in the rotating frame, and the above discussion was certainly not meant as an attempt to lead NMR spectroscopists away from that practice. However, I assert that grasping the magnetic resonance phenomenon directly in the stationary frame without first plunging into the rotating frame gives a

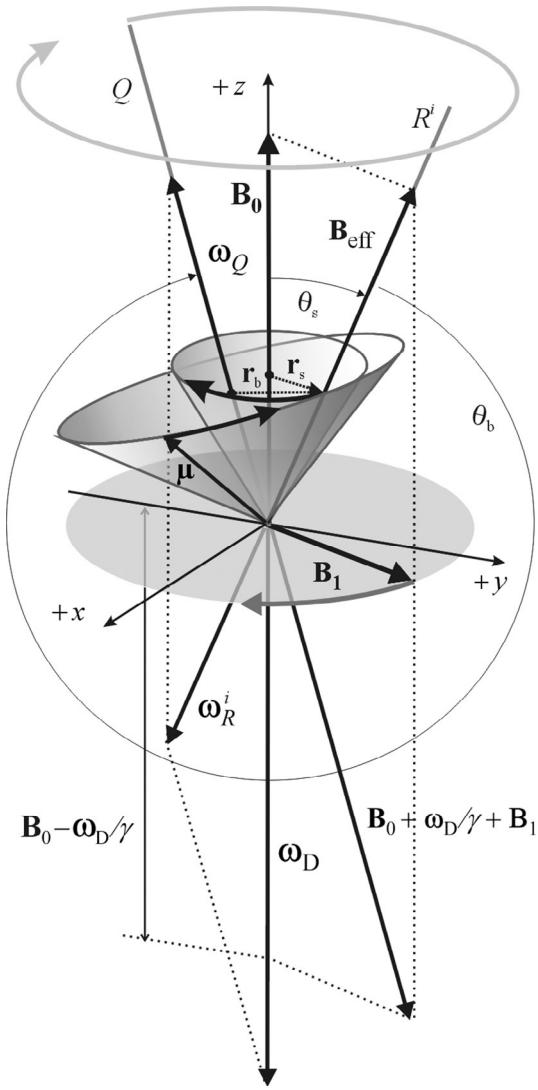

FIGURE 2.7 Conceptual illustration of the motion of an isolated magnetic moment $\boldsymbol{\mu}$ in the laboratory frame in a $\mathbf{B}_0$ static field and a $\mathbf{B}_1$ driving field rotating in the (x,y) plane for the off-resonance case when $\omega_D > \omega_0$. In reality, $B_1 \ll B_0$, and therefore $\theta_s \approx 0$. This is a case of a concave body cone rolling on the outside of a convex space cone; the body cone exhibits retrograde rotation.

fuller and "healthier" understanding of NMR, even if subsequently one falls into the usual and convenient routine of thinking within the rotating frame.

2.4 CLASSICAL PORTRAYAL OF THE MACROSCOPIC MAGNETIZATION

Having gained some initial idea about how spins *would* behave under the conditions of magnetic resonance *if* they behaved as classical objects, we now turn our attention to how an ensemble of spins behaves in the presence of the $\mathbf{B}_0$ and $\mathbf{B}_1$ fields. In particular, we are

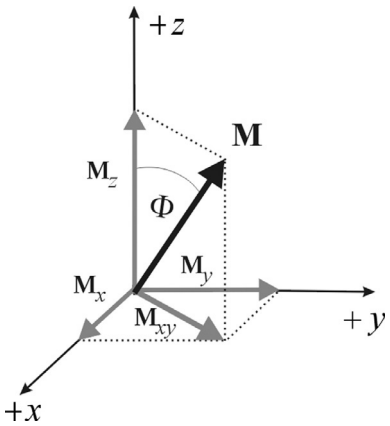

FIGURE 2.8 General depiction of the macroscopic magnetization **M** in the 3D-coordinate system.

interested in the prospect of the vector sum of the $\boldsymbol{\mu}$ moment vectors in the ensemble giving a non-zero vector $\sum\boldsymbol{\mu} = \mathbf{M}$, which we call the *macroscopic magnetization* of the ensemble.

In general, it will be convenient to treat **M** in our usual coordinate system as shown in Fig. 2.8. For convenience the projection of **M** onto the transversal plane is denoted as $\mathbf{M}_{xy}$, where $M_{xy} = \sqrt{M_x^2 + M_y^2}$. The angle between **M** and the $+z$ axis is Φ.

Where does this macroscopic magnetization come from in a $\mathbf{B}_0$ field? In the absence of an external magnetic field the $\boldsymbol{\mu}$ moment vectors in the ensemble are of course oriented randomly in 3D space, giving a kind of "spin-globe" if we imagine that all $\boldsymbol{\mu}$ vectors are shifted into the origin of the system as represented in Fig. 2.9a. Because we have a very large number of spins in the ensemble, in this case $\sum\boldsymbol{\mu} = \mathbf{0}$ at any given instant. If we now imagine suddenly placing the ensemble in a $\mathbf{B}_0$ field, intuition suggests that, similarly to the way a compass needle aligns itself along Earth's magnetic field in order to minimize its magnetic potential energy, the $\boldsymbol{\mu}$ moment vectors will likewise try to orient themselves toward the direction of $\mathbf{B}_0$ (i.e., to decrease θ) in order to decrease their potential energy (Eq. 2.3). However, according to Eq. (2.7) each $\boldsymbol{\mu}$ vector will start to Larmor-precess about the field according to Fig. 2.2, tracing a cone with the specific θ angle that the spin happened to have in the instant that $\mathbf{B}_0$ was "turned on," and will therefore not be able to lose potential energy. On this basis, we should initially expect that the $\sum\boldsymbol{\mu} = \mathbf{0}$ condition will be maintained. In reality however, after a few seconds the ensemble will become slightly polarized toward the direction of the $\mathbf{B}_0$ field, creating a net equilibrium magnetization $\sum\boldsymbol{\mu} = \mathbf{M}^{\mathrm{eq}} = M^{\mathrm{eq}}\mathbf{e}_z$; $M_{xy} = 0$, as illustrated in Fig. 2.9b. It should be noted that the degree of the polarization of the $\boldsymbol{\mu}$ vectors is, qualitatively speaking, extremely small, that is, M^{eq} is a very small value even at high magnetic fields, which is why NMR is an inherently insensitive spectroscopic method.

The "hedgehog" image of the spin ensemble as shown in Fig. 2.9 represents a sound metaphoric pictorial model of the spins and the microscopic constitution of the macroscopic magnetization which, as we shall see in Chapter 3, is physically relevant both classically and quantum-mechanically. This picture of the spin ensemble is critically important: it reflects a physically sound pictorial description of spins in a magnetic field and helps greatly to form a

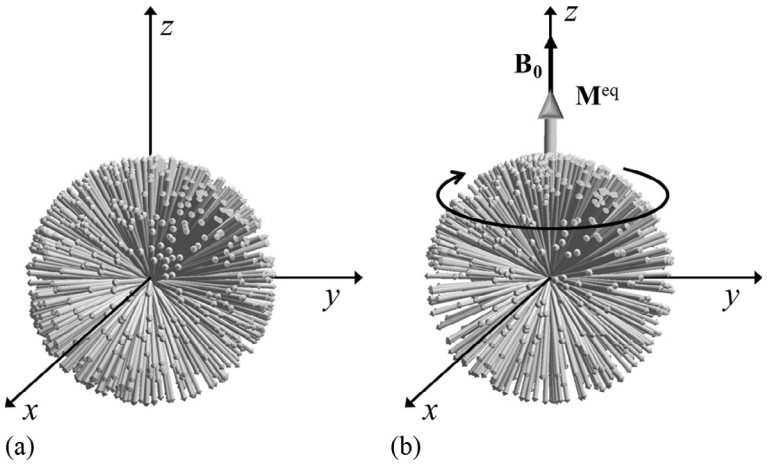

FIGURE 2.9 Very weekly interacting ensemble of classical $\boldsymbol{\mu}$ magnetic moment vectors (represented as "needles") shifted into the origin of the 3D-coordinate system. (a) Ensemble in the absence of an external magnetic field, forming a "spin-globe" in which the $\boldsymbol{\mu}$ vectors are distributed evenly. (b) Ensemble in the presence of the $\mathbf{B}_0$ static field following the establishment of thermal equilibrium with the environment (spin-lattice relaxation); the $\boldsymbol{\mu}$ vectors show a slight polarization toward $\mathbf{B}_0$, with their vector sum giving rise to a net equilibrium magnetization $\mathbf{M}^{eq} = M^{eq}\mathbf{e}_z$. Individual spins are precessing with the Larmor frequency as indicated by the curved arrow, while they are occasionally also exchanging energy among themselves (spin-spin relaxation). *The 3D illustrations of the "hedgehog-like" distributions of spins shown in the figures were taken from, and modified for the present discussion, Ref. 1 by permission of John Wiley& Sons.*

humanly tangible mental image of their behavior thus providing the basis of a good intuitive understanding of many NMR phenomena such as relaxation and coherence.

The process through which the system goes from the state $\sum\boldsymbol{\mu} = \mathbf{0}$ (Fig. 2.9a) to $\sum\boldsymbol{\mu} = \mathbf{M}^{eq}$ (Fig. 2.9b) is called spin-lattice, longitudinal, or T_1 relaxation. More generally speaking, if by perturbing the system via an RF field (see below) we create a situation where we have a macroscopic magnetization $\mathbf{M}$ which points in an arbitrary direction so that $M_z < M^{eq}$ and $M_{xy} > 0$ as shown in Fig. 2.8, then if the perturbing influence is removed, the system will relax back into its equilibrium position as shown in Fig. 2.9b. In this more general scheme, besides the longitudinal relaxation process $M_z \longrightarrow M^{eq}$ we have a transversal decaying process $M_{xy} \longrightarrow 0$, called transversal or T_2 relaxation.

Spin-lattice relaxation is an exponential process described by the equations

$$\frac{d\mathbf{M}_z}{dt} = \frac{\mathbf{M}^{eq} - \mathbf{M}_z}{T_1} \tag{2.21a}$$

$$M^{eq} - M_z = \left(M^{eq} - M_z^{t=0}\right) \cdot e^{\frac{-t}{T_1}}, \tag{2.21b}$$

where $M_z^{t=0}$ is the longitudinal non-equilibrium magnetization at $t = 0$, that is, at the time when we start observing the development of the M_z component, and the time-constant T_1 is called the spin-lattice relaxation time.

Transversal relaxation is also an exponential process described as

$$\frac{d\mathbf{M}_{xy}}{dt} = -\frac{\mathbf{M}_{xy}}{T_2} \tag{2.22a}$$

$$M_{xy} = M_{xy}^{t=0} \cdot e^{\frac{-t}{T_2}}, \tag{2.22b}$$

where the time-constant T_2 is the transversal relaxation time.

NMR relaxation theory is a rather intriguing and difficult topic in its own right. Relaxation theorists are (more or less) a subspecies of NMR spectroscopists, and in that respect NMR people may be divided (more or less) into two groups: those who have a detailed knowledge of relaxation based on some heavy mathematics, and those who simply take relaxation for granted without getting involved in how or why it happens. Indeed, many NMR spectroscopists can "live and breathe" NMR in a most constructive and fruitful manner without understanding relaxation very much beyond the phenomenological level represented by Eqs. (2.21a), (2.21b), (2.22a), and (2.22b), and by succumbing merrily to a cursory explanation such as the following. "T_1 relaxation occurs because the $\mathbf{B}_0$ field tries to orient the $\boldsymbol{\mu}$ moment vectors toward itself, thereby decreasing the energy of the ensemble, while this process is counteracted by the thermal agitation of the system which tries to randomize the spins; the 'relaxed' state represents an equilibrium between these two processes. T_2 relaxation occurs because in the absence of an orienting field in the (x,y) plane, the randomization process prevails." This is an intuitively attractive description (cf. Trap #10) which certainly has elements of truth, but if one starts scratching below the surface, some interesting questions emerge (e.g., according to Eq. (2.5) the $\mathbf{B}_0$ field does not "pull" the spins toward itself but makes them precess; also, it is not clear how exactly Brownian motion can influence the orientation of the spins, etc.). Addressing such questions reveals that the (synoptic) understanding of relaxation requires dealing with some counter-intuitive concepts, which however lead to some Aha!-type insights into the nature of relaxation. These aspects of relaxation are, at the very least, *nice* to know (cf. Pillar 15). Below is a brief attempt to approach relaxation in such a synoptic manner.

Note, first of all, that the concept of relaxation is applicable only to the macroscopic magnetization $\mathbf{M}$. It is not possible to speak of the relaxation of a single spin. We need to keep this in mind when attempting to conceptualize the microscopic mechanism of relaxation at the level of only a few spins, as discussed below.

Because in the absence of the $\mathbf{B}_0$ field spins are distributed uniformly within the spin-globe (Fig. 2.9a), in the instant when we "turn on" the $\mathbf{B}_0$ field the total potential energy $\sum E_\mu^{\text{pot}}$ of the ensemble is zero according to Eq. (2.3). The fact that after a while the system exhibits a net equilibrium magnetization $\mathbf{M}^{\text{eq}}$ means that the Northern hemisphere of the spin-globe has become more densely populated with spins than the Southern hemisphere (Fig. 2.9b), that is, the total energy $\sum E_\mu^{\text{pot}}$ has *decreased* slightly relative to that in the absence of $\mathbf{B}_0$; in other words the system has *relaxed* into a lower energy state than it was in when the $\mathbf{B}_0$ field appeared. This process raises several interesting questions, such as: how can we explain the decrease in the average θ value of the spins in light of the θ-conserving nature of the Larmor precession? Where does the lost energy go? What determines the degree of loss in $\sum E_\mu^{\text{pot}}$, that is, the magnitude of $\mathbf{M}^{\text{eq}}$?

The first step in answering these questions is to note that the spin ensemble is not "alone": in our model the proton spins form pairs in an H_2O molecule. This is significant for two

reasons. First, the spins of a spin-pair are close enough to each other to feel each other's local magnetic field, denoted herein as $\boldsymbol{\ell}$. Secondly, water molecules undergo continuous rapid and random Brownian motion, whereby the relative position of the spins in a spin-pair constantly changes, creating randomly fluctuating $\boldsymbol{\ell}$ fields at each other's site. The situation is illustrated for a pair of magnetic moments $\boldsymbol{\mu}_j$ and $\boldsymbol{\mu}_k$, generating the fluctuating local fields $\boldsymbol{\ell}_j(t)$ and $\boldsymbol{\ell}_k(t)$, in Fig. 2.10.

With the above notions in mind, the essence of relaxation can be understood by taking some fundamental principles of statistical thermodynamics[7] and applying them to our spin ensemble model (note that it is not at all easy to do this with a view to keeping our description and understanding at a synoptic level). In particular, it should be realized that from a statistical-thermodynamical point of view the spin ensemble is not an isolated system, but is coupled to another system, namely a thermal reservoir (the "lattice") characterized by the kinetic energy of the water molecules due to their Brownian motion. Let us simplify as well as specify the situation so as to facilitate intuitive understanding. Because of the Brownian motion the molecules continually collide and thus exchange rotational energy, so at any instant a given water molecule rotates with an instantaneous angular frequency $\boldsymbol{\omega}_{\text{mol}}^{\text{rot}}$. We assume that the molecules behave as rigid rotors and tumble isotropically in 3D space, therefore all directions of rotation are equally possible as illustrated conceptually in Fig. 2.11. Classically the rotational energy $E_{\text{mol}}^{\text{rot}}$ of a molecule is proportional to $(\omega_{\text{mol}}^{\text{rot}})^2$. In reality $E_{\text{mol}}^{\text{rot}}$ is of course quantized according to the quantized rotational states of a molecule. One may choose to keep this aspect in mind during the following discussion, but is has no particular relevance with regard to our main theme of understanding what statistical rules drive relaxation. The total rotational energy $\sum E_{\text{mol}}^{\text{rot}}$ of the molecular ensemble is distributed among the molecules according to statistical physics principles. By "lattice" we mean the sum of these rotational energies. In a 3D angular-velocity vector space the angular velocities of the

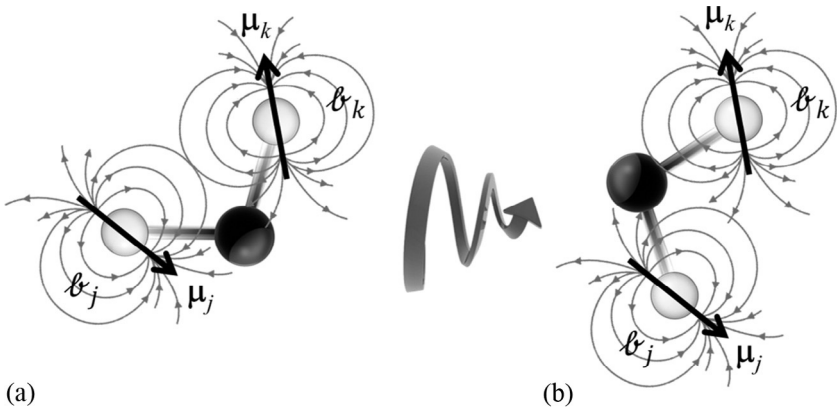

FIGURE 2.10 Schematic illustration of the way the two magnetic moments, $\boldsymbol{\mu}_j$ and $\boldsymbol{\mu}_k$, of the protons in a water molecule "sense" each other's fluctuating local fields $\boldsymbol{\ell}_j$ and $\boldsymbol{\ell}_k$ that arise as a result of the Brownian motion of the molecule. For simplicity, in this figure the (arbitrary) orientations of $\boldsymbol{\mu}_j$ and $\boldsymbol{\mu}_k$ were kept constant as the molecule has rotated from (a) to (b), so as to illustrate more directly the phenomenon that in (a) $\boldsymbol{\mu}_j$ is located in a different position of the magnetic field-line map of $\boldsymbol{\mu}_k$ than in (b), therefore $\boldsymbol{\mu}_j$ feels a randomly fluctuating field $\boldsymbol{\ell}_k$ coming from $\boldsymbol{\mu}_k$ (the same goes for the way $\boldsymbol{\mu}_k$ feels $\boldsymbol{\mu}_j$ of course). In reality, in a $\mathbf{B_0}$ field both spins also undergo Larmor precession (not shown) which also contributes to $\boldsymbol{\ell}_j$ and $\boldsymbol{\ell}_k$.

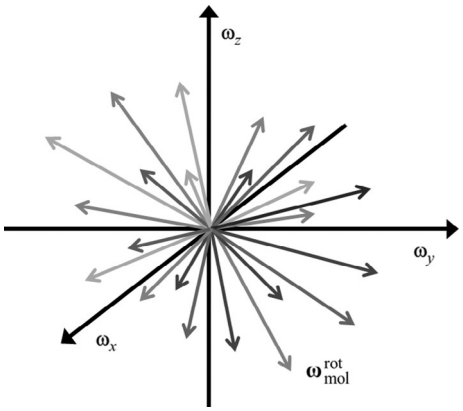

FIGURE 2.11 Schematic illustration of the distribution of the angular-velocity vectors (all brought into the origin) of isotropically rotating water molecules in 3D angular-velocity space.

water molecules may be assumed to be distributed according to Maxwell-Boltzmann statistics, in analogy with the well-known Maxwell distribution of linear velocities in an ideal gas (this is just a conceptual approximation, the exact shape of the distribution is irrelevant in the present context).

In a $\mathbf{B}_0$ field the spin ensemble and the lattice represent two different forms of energy, the potential energy $\sum E_{\mu}^{\text{pot}}$ and the rotational energy $\sum E_{\text{mol}}^{\text{rot}}$. Spin-lattice relaxation is about the way the spin ensemble exchanges energy with the lattice such that when the former loses energy, this is dissipated into the lattice in the form of a tiny amount of heat by increasing its energy $\sum E_{\text{mol}}^{\text{rot}}$ slightly. The macroscopic magnetization $\mathbf{M}^{\text{eq}}$ represents the state when the spin ensemble and the lattice have attained a state of thermal equilibrium. In order to see how this happens, we need to further specify the model of the spin-lattice system through the following simplifying assumptions. (1) The total system is isolated, therefore the total energy of the combined spin-lattice system E_{total} is constant. (2) The spin ensemble and the lattice are free to exchange energy. (3) There is only a weak contact between the two systems, therefore their energies are additive, that is, $E_{\text{total}} = \sum E_{\mu}^{\text{pot}} + \sum E_{\text{mol}}^{\text{rot}}$. (4) The spin ensemble and the lattice relate to each other as a *small* and a *large* macroscopic system, meaning that the latter has many more degrees of freedom than the former (a system having f degrees of freedom means that f independent physical parameters are needed to specify each possible state of the system). For this reason, the lattice acts as a thermodynamic heat reservoir against the spin ensemble, which means that no matter how much energy flows into it in the form of heat from the spin ensemble, its temperature will only increase negligibly.

As already noted, the transfer of energy between the spin ensemble and the lattice, and also within the spin ensemble, is made possible by the local fluctuating fields $\boldsymbol{\ell}$. To see how, let us reduce in thought the situation again to the magnetic moments $\boldsymbol{\mu}_j$ and $\boldsymbol{\mu}_k$ situated in a single water molecule as shown in Fig. 2.10, and let us assume that within a short examined interval of time the sum of the energies $E_{\mu(j)}^{\text{pot}} + E_{\mu(k)}^{\text{pot}} + E_{\text{mol}}^{\text{rot}}$ may be regarded as constant. If Larmor precession is also taken into account, the local field $\boldsymbol{\ell}_k$ generated by $\boldsymbol{\mu}_k$ will contain a fluctuating transversal field $\boldsymbol{\ell}_{xy(k)}$ which also contains a component rotating with the Larmor frequency, and a longitudinal field $\boldsymbol{\ell}_{z(k)}$ fluctuating according to the rotational motion of the water molecule (transversal motion also counts here but we ignore that for simplicity). From the

considerations represented in Fig. 2.2, it is easy to see that the fluctuating $\boldsymbol{\ell}_{z(k)}$ field either slightly increases or slightly decreases the Larmor frequency $\omega_{0(j)} = \gamma B_0$ of $\boldsymbol{\mu}_j$ (depending on whether, at a given instant, $\boldsymbol{\ell}_{z(k)}$ is parallel or antiparallel with $\mathbf{B}_0$), but does not change the potential energy of the system. Because this process gives rise to slightly different precession frequencies in the spin ensemble, it causes a dephasing of the spins in the (x,y) plane, thus contributing to T_2 relaxation (cf. Eqs. 2.22a and 2.22b).

As for the $\boldsymbol{\ell}_{xy(k)}$ field, because it rotates in the transverse plane at the Larmor frequency of $\boldsymbol{\mu}_j$, it will induce a kind of "microresonance" on $\boldsymbol{\mu}_j$, either increasing or decreasing slightly its potential energy $E^{\text{pot}}_{\mu(j)}$ (note that, as opposed to $B_1(t)$, $\boldsymbol{\ell}_{xy(k)}$ contains randomly varying components due to molecular tumbling). If, say, $E^{\text{pot}}_{\mu(j)}$ slightly *increases*, one of two things can happen. One possibility is that $\boldsymbol{\mu}_k$ simultaneously *decreases* its $E^{\text{pot}}_{\mu(k)}$ potential energy to the same degree under the influence of the fluctuating field $\boldsymbol{\ell}_{xy(j)}$due to $\boldsymbol{\mu}_j$ (one should not forget that $\boldsymbol{\mu}_k$ affects $\boldsymbol{\mu}_j$ the same way as vice versa). Thus, there is a mutual exchange of energy between $\boldsymbol{\mu}_j$ and $\boldsymbol{\mu}_k$ in the process, leaving their total potential energy intact—this process is also a T_2 relaxation mechanism.

The second thing that can happen when $E^{\text{pot}}_{\mu(j)}$ slightly increases due to a "micro-resonance" of $\boldsymbol{\mu}_j$ is that this increase in $E^{\text{pot}}_{\mu(j)}$ is compensated by an appropriate decrease in $E^{\text{rot}}_{\text{mol}}$, that is, the molecular rotation slows down a tiny bit—in other words, a bit of heat flows from the lattice into the spin-system. Conversely, if $E^{\text{pot}}_{\mu(j)}$ happens to decrease as a result of a micro-resonance of $\boldsymbol{\mu}_j$, then the "price" of this energy loss can be a slight increase in the angular velocity of the molecule, that is, in a slight increase of the heat of the lattice. Extending this concept to the interaction of the whole spin ensemble and the lattice, we see that this process provides a mechanism for energy exchange between the two systems, which is the basis of T_1 relaxation:

$$\sum E^{\text{pot}}_{\mu} \overset{\boldsymbol{\ell}(t)}{\longleftrightarrow} \sum E^{\text{rot}}_{\text{mol}}. \tag{2.23}$$

From all this, we see that both the spin ensemble and the lattice are statistical ensembles. Within each system the members of the ensemble are continually exchanging energies, which means that in Fig. 2.9 the individual spin vectors constantly change their longitudinal and latitudinal positions on the surface of the spin-globe (while maintaining their Larmor precession), and in Fig. 2.11 the angular-velocity vector of each molecule changes direction and magnitude according to the assumed Maxwell distribution. Also, there is a constant energy transfer to and fro between the two systems. Energy exchange between the spins does not affect the total energy $\sum E^{\text{pot}}_{\mu}$ of the spin ensemble, that is, it does not explain the development of $\mathbf{M}^{\text{eq}}$. The latter requires that $\sum E^{\text{pot}}_{\mu}$ must decrease to a certain extent, and from (2.23) this is possible only if a certain amount of energy flows from $\sum E^{\text{pot}}_{\mu}$ into $\sum E^{\text{rot}}_{\text{mol}}$. The question is, what "motivates" the spin ensemble, when placed in a $\mathbf{B}_0$ field, to give up some of its potential energy to the lattice, and what determines the degree to which it will do so?

These questions bring us to the very important and interesting concepts of the *macrostates* and *microstates* of a system. Let us, in that respect, consider again our "hedgehog" distribution of spins shown in Fig. 2.9. Imagine that we divide the surface of the spin-globe into small equal surface elements (cells), such as the hexagons shown in Fig. 2.12. The cells are assumed to be small enough so that within a given cell the energy E^{pot}_{μ} may be regarded as constant (in that respect, Fig. 2.12 exaggerates the cells for illustrative purposes).

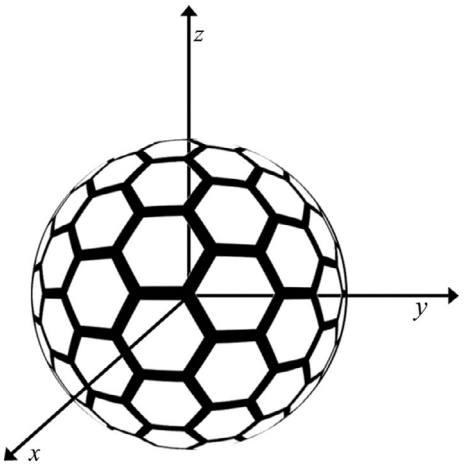

FIGURE 2.12 The concept of dividing the surface of the spin-globe into small equal surface elements (cells) such as the hexagons shown here.

Let us now take our spin ensemble as shown in Fig. 2.9a, assuming initially that there is no $\mathbf{B}_0$ field (there is no potential energy associated with the spins). Imagine that we pick out, say, two water molecules, that is, four specific moment vectors, and let us label them individually as $\boldsymbol{\mu}_1$, $\boldsymbol{\mu}_2$, $\boldsymbol{\mu}_3$, and $\boldsymbol{\mu}_4$ (just for a while we ignore the rest of the spins). Now let us choose *any* four *different* cells in Fig. 2.12, and label them in some convenient way, say as cell_a, cell_b, cell_c, and cell_d. The tips of the moment vectors will keep moving randomly on the surface of the spin-globe, which means that in time $\boldsymbol{\mu}_1$ may be found with equal probability in cell_a, cell_b, cell_c, and cell_d. The same is true of course for $\boldsymbol{\mu}_2$, $\boldsymbol{\mu}_3$, and $\boldsymbol{\mu}_4$. Let us specify *which* particular spin occupies *which* particular cell in a given instant. For example, we may have $\boldsymbol{\mu}_1$ and $\boldsymbol{\mu}_3$ in cell_a, no spin in cell_b, $\boldsymbol{\mu}_4$ in cell_c, and $\boldsymbol{\mu}_2$ in cell_d, which is a microscopic configuration of the system that I will denote here as $\{\boldsymbol{\mu}_1,\boldsymbol{\mu}_3@\text{cell}_a;\ \boldsymbol{\mu}_4@\text{cell}_c;\ \boldsymbol{\mu}_2@\text{cell}_d\}$. Such an instantaneous microscopic configuration, that is, when we know which individual spin is located in which individual cell, is called a *microstate* of the system. For example, the states $\{\boldsymbol{\mu}_1,\boldsymbol{\mu}_2,\boldsymbol{\mu}_3,\boldsymbol{\mu}_4@\text{cell}_a\}$ and $\{\boldsymbol{\mu}_3@\text{cell}_a;\ \boldsymbol{\mu}_1@\text{cell}_b;\ \boldsymbol{\mu}_4@\text{cell}_c;\ \boldsymbol{\mu}_2@\text{cell}_d\}$ are different microstates of this system. As far as the macroscopic behavior of the spin ensemble is concerned, it is of course indifferent which spin occupies which cell, all that matters is how many spins are located in a given cell. The state of the system characterized by the *number* of spins found in the individual cells is called the *macrostate* of the system. For example, the states $\{\boldsymbol{\mu},\boldsymbol{\mu},\boldsymbol{\mu},\boldsymbol{\mu}@\text{cell}_a\}$ and $\{\boldsymbol{\mu}@\text{cell}_a;\ \boldsymbol{\mu}@\text{cell}_b;\ \boldsymbol{\mu}@\text{cell}_c;\ \boldsymbol{\mu}@\text{cell}_d\}$ represent different macrostates of the system. A fundamental principle of statistical thermodynamics, known as the *postulate of equal a priori probabilities*, states that an isolated system in equilibrium is equally likely to be in any of its accessible microstates. This means that the probability of finding the system in microstate $\{\boldsymbol{\mu}_1,\boldsymbol{\mu}_2,\boldsymbol{\mu}_3,\boldsymbol{\mu}_4@\text{cell}_a\}$ is the same as the probability of finding it in the microstate $\{\boldsymbol{\mu}_3@\text{cell}_a;\ \boldsymbol{\mu}_1@\text{cell}_b;\ \boldsymbol{\mu}_4@\text{cell}_c;\ \boldsymbol{\mu}_2@\text{cell}_d\}$ or $\{\boldsymbol{\mu}_3,\boldsymbol{\mu}_4@\text{cell}_a;\ \boldsymbol{\mu}_1@\text{cell}_b;\ \boldsymbol{\mu}_2@\text{cell}_d\}$, etc. Note however that the macrostate $\{\boldsymbol{\mu}@\text{cell}_a;\ \boldsymbol{\mu}@\text{cell}_b;\ \boldsymbol{\mu}@\text{cell}_c;\ \boldsymbol{\mu}@\text{cell}_d\}$ corresponds to $4! = 24$ different microstates (all possible permutations according to which $\boldsymbol{\mu}_1$, $\boldsymbol{\mu}_2$, $\boldsymbol{\mu}_3$, and $\boldsymbol{\mu}_4$ can occupy the cells in a one-to-one arrangement), whereas the macrostate $\{\boldsymbol{\mu},\boldsymbol{\mu},\boldsymbol{\mu},\boldsymbol{\mu}@\text{cell}_a\}$ corresponds of course to only one microstate, $\{\boldsymbol{\mu}_1,\boldsymbol{\mu}_2,\boldsymbol{\mu}_3,\boldsymbol{\mu}_4@\text{cell}_a\}$. This means that while all microstates are equally probable, finding the

system in a macrostate of {$\boldsymbol{\mu}$@cell$_a$; $\boldsymbol{\mu}$@cell$_b$; $\boldsymbol{\mu}$@cell$_c$; $\boldsymbol{\mu}$-@cell$_d$} is 24 times more probable than finding it in the macrostate {$\boldsymbol{\mu}$,$\boldsymbol{\mu}$,$\boldsymbol{\mu}$,$\boldsymbol{\mu}$@cell$_a$}. This example illustrates the general rule that *the probability of any macrostate is proportional to the number of microstates accessible to that macrostate*. Clearly, if we take more spins into account, the number of microstates compatible with a macrostate in which each spin is situated in a different cell increases rapidly. On that basis, the argument can be readily extended to the whole spin ensemble. If, for simplicity, we imagine that we have the same number of cells as spins, and each spin is individually labeled, then a microstate where we find all of the spins in any single given cell is equally probable as a microstate where spins are evenly distributed on the surface such that each cell with a known location is occupied by a single spin with a known label (Fig. 2.9a). Clearly, there will be a very huge number of microstates that give the same macrostate for this evenly distributed arrangement, while any other configuration, such as the all-spins-in-a-single-cell macrostate, will have far less accessible microstates, and will thus be much less likely to occur.

An entirely analogous argument applies to the lattice, except that in Fig. 2.11 the angular-velocity vectors do not have a fixed length. As noted above, for argument's sake we may assume a Maxwell distribution of angular velocities. This means that along any given spatial direction the angular velocities follow a Boltzmann distribution (i.e., smaller rotational frequencies with smaller energies are more probable), but if all possible spatial directions are taken into account, then the probability of finding a molecule in the small range $\omega_{\text{mol}}^{\text{rot}} + \delta\omega_{\text{mol}}^{\text{rot}}$, irrespective of its direction of rotation, goes through a maximum. To see why, imagine that we divide the entire angular-velocity space shown in Fig. 2.11 into a 3D grid of very small volume elements (voxels), with each voxel covering the range $\omega_{\text{mol}(x)}^{\text{rot}}$ to $\omega_{\text{mol}(x)}^{\text{rot}} + \delta\omega_{\text{mol}(x)}^{\text{rot}}$, $\omega_{\text{mol}(y)}^{\text{rot}}$ to $\omega_{\text{mol}(y)}^{\text{rot}} + \delta\omega_{\text{mol}(y)}^{\text{rot}}$, and $\omega_{\text{mol}(z)}^{\text{rot}}$ to $\omega_{\text{mol}(z)}^{\text{rot}} + \delta\omega_{\text{mol}(z)}^{\text{rot}}$. Let us now, in order to simplify illustration, look onto, say, the 2D (z,x) plane of the angular-velocity space shown in Fig. 2.11, and also for simplicity, let us, in this plane, represent as a dot the tip of each $\boldsymbol{\omega}_{\text{mol}}^{\text{rot}}$ vector. Accordingly, the distribution of angular velocities in the lattice at thermal equilibrium will look something like that shown in Fig. 2.13.

It is easy to appreciate from Fig. 2.13 that if we draw a straight line in any arbitrarily chosen direction from the origin, then the probability of finding molecules whose rotational axes

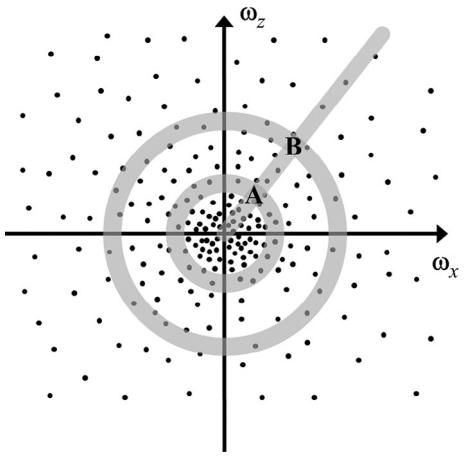

FIGURE 2.13 Conceptual illustration of the most probable macrostate according to which molecular angular velocities are distributed in the lattice at thermal equilibrium, as represented in a 2D slice of angular-velocity space. The dots indicate the tips of the angular-velocity vectors starting from the origin (cf. Fig. 2.11). The shaded line represents an arbitrarily chosen linear series of voxels starting from the origin, along which molecules are distributed according to Boltzmann's formula. The shaded circles denote the 2D slices of two spherical shells of a single layer of voxels that have the same rotational energy.

point in (almost) the same direction decreases with increasing angular frequency, that is, with increasing energy $E^{\text{rot}}_{\text{mol}}$. This is Boltzmann's distribution: it has a maximum value at the origin and drops exponentially with increasing energy. Thus, for example, finding a molecule which rotates at a speed and direction that corresponds to, say, voxel A in Fig. 2.13 is more likely than finding it in voxel B. If however we take into account all possible rotational directions, that is, all of the accessible microstates that belong to a given energy, a different situation emerges. The shaded circles in Fig. 2.13 illustrate this point. They represent the 2D slices of two spherical shells of arbitrarily chosen radius which contain all those voxels that have the same energy between the narrow range $E^{\text{rot}}_{\text{mol}}$ and $E^{\text{rot}}_{\text{mol}} + \delta E^{\text{rot}}_{\text{mol}}$ (each shell is as thick as a single voxel). We see from this that although for a given molecule state A is more likely than state B, there are a lot more voxels that have the same energy as state B than there are that have the same energy as state A. In other words, there are many more accessible microstates for higher energy molecules than for lower energy ones (recall that the volume of a sphere increases with the cube of the sphere's radius). Thus, from a macroscopic viewpoint, in which case we are only interested in the *number* of molecules that have a given rotational energy, the distribution of rotational speeds will be determined by two competing factors: with increasing energy, single voxels will be less densely populated (this factor decreases the probability of molecules being in a higher energy rotational state), but at the same time the number of voxels compatible with a given energy will increase (this factor increases the probability of molecules being in a higher energy molecular state). A Maxwell-type distribution of angular speeds ensues: macroscopically the distribution function is zero at the origin, then goes through a maximum and diminishes toward zero with increasing energies.

Now that we have a feel for macrostates and microstates in both the spin ensemble and the lattice, we need to bring the two systems together and think about it as a *combined* spin ensemble + lattice system in order to understand the reason why the spin ensemble develops an equilibrium macroscopic magnetization $\sum \boldsymbol{\mu} = \mathbf{M}^{\text{eq}}$ in a $\mathbf{B}_0$ field. To that end, we need to make an additional important observation regarding the behavior of such a combined system. Recall, first, our initial premise that the energies of the respective systems are additive and their sum is a constant:

$$E_{\text{total}} = \sum E^{\text{pot}}_{\mu} + \sum E^{\text{rot}}_{\text{mol}}. \tag{2.24}$$

From the above considerations, we should intuitively expect that the combined system will also be most likely found in a state which has the largest number of microstates accessible to the system as a whole. With that in mind, we want to look for the most probable energy $\sum E^{\text{pot}}_{\mu}$ of the spin ensemble that ensures that the combined system has the maximum number of accessible microstates. Adopting, along with some of his argument, the symbol Ω used by F. Reif to indicate the number of microstates,[8] let us denote by $\Omega_{\text{total}}\left(\sum E^{\text{pot}}_{\mu}\right)$ the number of microstates accessible to the combined system if the spin ensemble has an energy $\sum E^{\text{pot}}_{\mu}$ (or more precisely, very nearly that energy). According to the principle of *a priori* probabilities, at equilibrium all accessible microstates of the combined system are equally likely, consequently finding the spin ensemble to have an energy $\sum E^{\text{pot}}_{\mu}$ is proportional to the number of microstates $\Omega_{\text{total}}\left(\sum E^{\text{pot}}_{\mu}\right)$ accessible to the combined system. However, if the spin ensemble has an energy $\sum E^{\text{pot}}_{\mu}$, it can be in any one of its own $\Omega_{\text{spins}}\left(\sum E^{\text{pot}}_{\mu}\right)$ microstates. From (2.23) we see

that at the same time the lattice has an energy $\sum E_{\text{mol}}^{\text{rot}} = E_{\text{total}} - \sum E_{\mu}^{\text{pot}}$, so it can be in any one of its $\Omega_{\text{lattice}}\left(\sum E_{\text{mol}}^{\text{rot}}\right) = \Omega_{\text{lattice}}\left(E_{\text{total}} - \sum E_{\mu}^{\text{pot}}\right)$ accessible microstates. Clearly, every possible microstate of the spin ensemble can be combined with every possible microstate of the lattice, and each combination will give a different microstate for the combined system, therefore the number of microstates $\Omega_{\text{total}}\left(\sum E_{\mu}^{\text{pot}}\right)$ accessible to the combined system when the spin ensemble has an energy $\sum E_{\mu}^{\text{pot}}$ will be the product

$$\Omega_{\text{total}}\left(\sum E_{\mu}^{\text{pot}}\right) = \Omega_{\text{spins}}\left(\sum E_{\mu}^{\text{pot}}\right)\Omega_{\text{lattice}}\left(\sum E_{\text{mol}}^{\text{rot}}\right), \tag{2.25}$$

and therefore the probability $P\left(\sum E_{\mu}^{\text{pot}}\right)$ of the spin ensemble having an energy $\sum E_{\mu}^{\text{pot}}$ is given by

$$P\left(\sum E_{\mu}^{\text{pot}}\right) \propto \Omega_{\text{spins}}\left(\sum E_{\mu}^{\text{pot}}\right)\Omega_{\text{lattice}}\left(\sum E_{\text{mol}}^{\text{rot}}\right). \tag{2.26}$$

Equation (2.26) holds the key to understanding why the spin ensemble polarizes itself to a certain degree toward the $\mathbf{B}_0$ field. Note that the number of accessible states for both the spin ensemble and the lattice increases very rapidly as a function of their energies because both systems have very many degrees of freedom f (in fact, $\Omega \propto E^f$). If $\sum E_{\mu}^{\text{pot}}$ *decreases* slightly, then the term $\Omega_{\text{spins}}\left(\sum E_{\mu}^{\text{pot}}\right)$ *decreases* extremely rapidly while the term $\Omega_{\text{lattice}}\left(\sum E_{\text{mol}}^{\text{rot}}\right) = \Omega_{\text{lattice}}\left(E_{\text{total}} - \sum E_{\mu}^{\text{pot}}\right)$ *increases* even more rapidly (because the lattice has many more degrees of freedom than the spin ensemble). The result is that the product of these two terms, that is, the probability $P\left(\sum E_{\mu}^{\text{pot}}\right)$ exhibits an extremely sharp maximum for some particular value of $\sum E_{\mu}^{\text{pot}}$, and this will be the most probable macrostate of the spin ensemble. Obviously, with reference to Eq. (2.3), the most probable energy $\sum E_{\mu}^{\text{pot}}$ will determine the extent to which the spin ensemble will become polarized toward the $\mathbf{B}_0$ field, and therefore the magnitude of the equilibrium macroscopic magnetization $\mathbf{M}^{\text{eq}}$.

We can illustrate the above conclusion in a semi-quantitative manner with some very small numbers (in which case the probability of the most probable macrostate will of course not have such a sharp maximum). Imagine that the spin ensemble has 240 microstates available when its energy is 0, expressed in arbitrary units, and we denote this condition as $[240(0)]_{\text{spins}}$. Assume, furthermore, that if the spin ensemble decreases its energy stepwise by single energy units, it will exhibit the following number of microstates: $[160(-1)]_{\text{spins}}$, $[90(-2)]_{\text{spins}}$, $[40(-3)]_{\text{spins}}$, $[10(-4)]_{\text{spins}}$. Now assume that the lattice has 10 units of rotational energy with 300 accessible microstates, that is, we have $[300(10)]_{\text{lattice}}$, and when we increase the energy of the lattice in one energy-unit steps, we obtain the following figures: $[800(11)]_{\text{lattice}}$, $[1600(2)]_{\text{lattice}}$, $[2600(13)]_{\text{lattice}}$, $[4000(14)]_{\text{lattice}}$. Let the total energy of the system be 10 units at equilibrium, which means that if the spin ensemble has 0 energy units, the lattice has 10 energy units, and by each energy unit that the spin ensemble "gives up," the energy of the lattice will increase by 1 unit. Under these circumstances, using Eq. (2.26) we obtain the following conceivable pairs of spin-lattice configurations and associated total number of microstates for the combined system:

$[240(0)]_{\text{spins}}$; $[300(10)]_{\text{lattice}} \rightarrow [72{,}000(10)]_{\text{total}}$
$[160(-1)]_{\text{spins}}$; $[800(11)]_{\text{lattice}} \rightarrow [128{,}000(10)]_{\text{total}}$

$[90(-2)]_{\text{spins}}$; $[1600(12)]_{\text{lattice}} \rightarrow [144{,}000(10)]_{\text{total}}$
$[40(-3)]_{\text{spins}}$; $[2600(13)]_{\text{lattice}} \rightarrow [104{,}000(10)]_{\text{total}}$
$[10(-4)]_{\text{spins}}$; $[4000(14)]_{\text{lattice}} \rightarrow [40{,}000(10)]_{\text{total}}$

We see from this simple example that if we suddenly place the spin ensemble in a $\mathbf{B}_0$ field so that it is imparted with a potential energy $\sum E_\mu^{\text{pot}}$, which at this instant is 0, then this will *not* be the most probable state of a spin ensemble at equilibrium with the lattice. The total system will achieve the maximum number of microstates if the spin ensemble gives up 2 units of potential energy and transfers it to the lattice's rotational energy, so this will be the most probable state of the spin ensemble (transferring more energy to the lattice would again decrease the total number of microstates). All this is illustrated pictorially in Fig. 2.14.

Figure 2.14a represents the situation when the $\mathbf{B}_0$ field is suddenly "turned on." At this instant our spin ensemble is as yet nonpolarized ($\sum \boldsymbol{\mu} = 0$), so we have very nearly the same number of spins in each cell on the surface of the spin-globe, corresponding to the maximum number of microstates available to the spin ensemble. The spin ensemble starts exchanging energy with the lattice, which at this instant has a certain number of microstates as suggested by the shaded globe in its angular-velocity space as shown in Fig. 2.14b. As per the previous argument, this however is not the most probable state of the spin ensemble with regard to the combined system. By letting some energy flow into the lattice, the spin ensemble will to some become polarized along $\mathbf{B}_0$ field ($\sum \boldsymbol{\mu} = \mathbf{M}$), that is, cells near the North pole of the spin-globe will become more densely populated by spins, therefore by this act the spin ensemble loses some of its microstates as shown in Fig. 2.14c. However, at the same time the lattice, due to its slightly increased energy, gains many more microstates (Fig. 2.14d), thereby increasing the probability of this polarized configuration of the spin ensemble according to Eq. (2.25). As described above, by giving up too much energy the spin ensemble will start losing too many

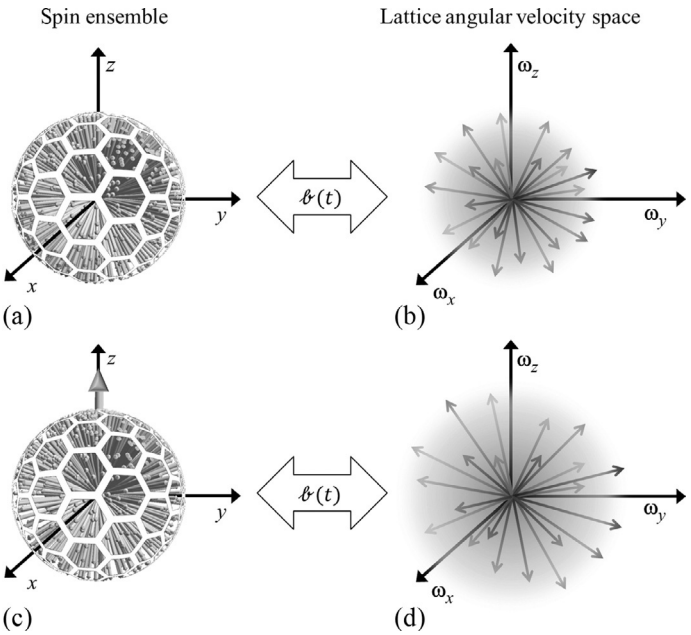

FIGURE 2.14 Conceptual illustration of how a nonpolarized spin ensemble becomes polarized due to its thermal interaction with the lattice, giving rise to the phenomenon of T_1 relaxation. (a) Macrostate of the nonpolarized spin ensemble at the moment when placed in a $\mathbf{B}_0$ field, having a maximum number of microstates and (b) simultaneous macrostate of the lattice in angular-velocity space, with a given number of microstates as indicated by the shaded globe. (c) Transferring some energy from the spin ensemble to the lattice results in some degree of polarization of the spins, whereby the number of microstates available to the spin ensemble decreases and (d) at the same time the number of microstates available to the lattice increases considerably, thereby this configuration of the combined system will be more probable according to Eq. (2.26).

microstates that will not be compensated by the associated gain in the number of lattice microstates as far as the product $\Omega_{\text{spins}}\left(\sum E_{\mu}^{\text{pot}}\right)\Omega_{\text{lattice}}\left(\sum E_{\text{mol}}^{\text{rot}}\right)$ is concerned, therefore at equilibrium a compromise is reached in the respective number of microstates which corresponds to the $\sum\boldsymbol{\mu} = \mathbf{M}^{\text{eq}}$ condition. This is the essential motivation behind T_1 relaxation.

Now that we have gained a sense of how and why a macroscopic magnetization $\mathbf{M}$ emerges from the spin ensemble from statistical considerations, we focus attention on how $\mathbf{M}$ behaves in the static $\mathbf{B}_0$ and rotating $\mathbf{B}_1$ fields. Note, first of all, that because of the *distributive* nature of both the vector product and the scalar product, that is, $\boldsymbol{\mu}_1 \times \mathbf{B} + \boldsymbol{\mu}_2 \times \mathbf{B} = (\boldsymbol{\mu}_1 + \boldsymbol{\mu}_2) \times \mathbf{B}$ and $\boldsymbol{\mu}_1 \cdot \mathbf{B} + \boldsymbol{\mu}_2 \cdot \mathbf{B} = (\boldsymbol{\mu}_1 + \boldsymbol{\mu}_2) \cdot \mathbf{B}$, Eqs. (2.1) and (2.3) can be readily applied to the macroscopic magnetization $\sum\boldsymbol{\mu} = \mathbf{M}$, that is, we have

$$\mathbf{T} = \mathbf{M} \times \mathbf{B} \text{ (i.e., } T = MB\sin\Theta) \tag{2.27}$$

$$E_M^{\text{pot}} = \sum E_{\mu}^{\text{pot}} = -\mathbf{M} \cdot \mathbf{B} = -MB\cos\Theta, \tag{2.28}$$

where Θ is the angle between $\mathbf{M}$ and $\mathbf{B}$. Using also Eqs. (2.2) and (2.4) under the understanding that $\sum\boldsymbol{\mu} = \gamma\sum\mathbf{P}$, the equation of motion (2.5) can be written for the macroscopic magnetization as

$$\frac{d\mathbf{M}}{dt} = \gamma[\mathbf{M} \times \mathbf{B}], \tag{2.29}$$

which tells us, of course, that $\mathbf{M}$ also precesses about the $\mathbf{B}$ field with a Larmor frequency of $\boldsymbol{\omega} = -\gamma\mathbf{B}$.

Note that we have arrived at Eqs. (2.27)–(2.29) by starting from Eqs. (2.1)–(2.5) and applying to them some simple and absolute mathematical truths. This however does not, in itself, guarantee the *physical* truth of Eqs. (2.27)–(2.29) (cf. Traps #11 and #12). When thinking this way (i.e., when going from a microscopic description to a macroscopic description), Eqs. (2.27)–(2.29) will be physically valid only to the extent that Eqs. (2.1)–(2.5) are physically valid. This, however, is not a *priori known* since we know that spins and atomic magnetic moments are quantum entities and not classical-physical objects. As it turns out, Eqs. (2.27)–(2.29) *do* indeed provide a sound description of physical reality, but this reflects a macroscopic physical truth which we may as well have "guessed" on classical-physical grounds without any prior microscopic considerations. Neither does the validity of Eqs. (2.27)–(2.29) per se follow from a microscopic physical truth of Eqs. (2.1)–(2.5), nor does it, by itself, indicate the physical correctness of Eqs. (2.1)–(2.5). As already noted in Section 2.3, the justification of using Eqs. (2.1)–(2.5) as a sound metaphoric description of the individual spin comes from quantum-mechanical considerations (see Chapter 3).

Based on the above ideas, we can combine Eq. (2.29) with Eqs. (2.21a), (2.21b), (2.22a), and (2.22b), which leads to the famous Bloch equation:

$$\frac{d\mathbf{M}}{dt} = \gamma[\mathbf{M} \times (\mathbf{B}_0 + \mathbf{B}_1(t))] + \frac{\mathbf{M}^{\text{eq}} - \mathbf{M}_z}{T_1} - \frac{\mathbf{M}_{xy}}{T_2} \tag{2.30}$$

wherein it will be of particular interest to note that the torque exerted upon $\mathbf{M}$ is due to the effective field $\mathbf{B}_{\text{eff}} = \mathbf{B}_0 + \mathbf{B}_1$.

We now want to consider what Eq. (2.30) tells us about the behavior of $\mathbf{M}$ during NMR excitation by the rotating $\mathbf{B}_1$ field. Using Eq. (2.12), Eq. (2.30) readily converts into the rotating frame as follows:

$$\left(\frac{d\mathbf{M}}{dt}\right)_{\text{rot}} = \gamma\left[\mathbf{M}\times\left(\mathbf{B}_0+\mathbf{B}_1+\frac{\boldsymbol{\omega}_D}{\gamma}\right)\right]+\frac{\mathbf{M}^{eq}-\mathbf{M}_z}{T_1}-\frac{\mathbf{M}_{x'y'}}{T_2}. \tag{2.31}$$

Let us assume that $\mathbf{B}_1$ is applied in the form of a short rectangular pulse, that is, it is suddenly turned on, has constant amplitude B_1 for a time Δt_{pulse} as viewed in the rotating frame, and then it is instantaneously turned off. In this case, under the on-resonance condition the flip angle Φ (cf. Fig. 2.8) is proportional to the duration of the pulse:

$$\Phi = \gamma B_1 \Delta t_{\text{pulse}} = \omega_1 \Delta t_{\text{pulse}}. \tag{2.32}$$

Figure 2.15b illustrates the situation when the torque $\mathbf{M}\times\mathbf{B}_{\text{eff}}^{\text{rot}} = \mathbf{M}\times\mathbf{B}_1$ drives $\mathbf{M}$ down to the $+y'$ axis (if the $\mathbf{B}_1$ field is chosen to be aligned along the $+x'$ axis), that is, $\Phi = 90°$, which is called a 90° pulse. The off-resonance conditions $\omega_D < \omega_0$ and $\omega_D > \omega_0$ are shown in Fig. 2.15a and c, respectively. Fig. 2.15a and c shows the off-resonance trajectories traced by $\mathbf{M}$ for $\omega_D < \omega_0$ and $\omega_D > \omega_0$, respectively, under the influence of the torque $\mathbf{M}\times\mathbf{B}_{\text{eff}}^{\text{rot}}$ when $\mathbf{B}_1$ is applied for the same length of time Δt_{pulse} as in Fig. 2.15b.

As another intricacy involving the rotating frame, consider the situation when $\mathbf{M}$ has been tilted away from the z axis by, say, a 90° resonant $\mathbf{B}_1$ pulse along the x' axis in the rotating frame, and the $\mathbf{B}_1$ field has just been turned off. If we remind ourselves of $\mathbf{M}$ being comprised of a spin ensemble (cf. Fig. 2.9), the situation can be represented as shown in Fig. 2.16. Note that in this process the individual spins do not change their relative orientation, therefore the magnitude of $\mathbf{M}$ does not change, that is, after the pulse it still has the value of M^{eq}.

At the instant of having turned off the $\mathbf{B}_1$ field, the spins distributed on the spin-globe are slightly polarized toward the y' axis, giving a transversal magnetization $\mathbf{M} = \mathbf{M}_{y'}$, but no longitudinal magnetization, that is, $M_z = 0$. Clearly, T_1 and T_2 relaxation must start to take effect in order to re-establish the equilibrium magnetization $M_z = M^{eq}$, $M_{x'y'} = 0$, whether or not we are

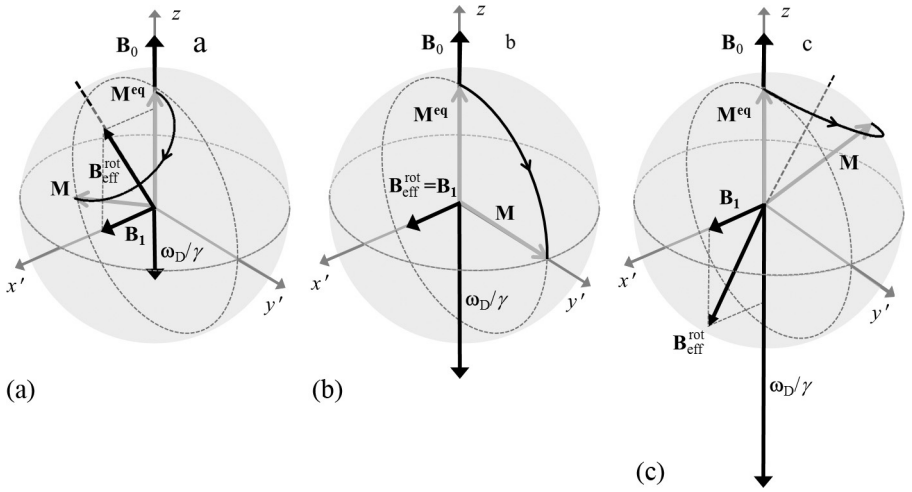

FIGURE 2.15 The trajectories traced by $\mathbf{M}$ in the rotating frame under off-resonance and on-resonance conditions. (a) $\omega_D < \omega_0$; (b) $\omega_D = \omega_0$; and (c) $\omega_D > \omega_0$. Case (b) illustrates the condition when $\mathbf{B}_1$ is applied in the form of a 90° pulse; in (a) and (c) $\mathbf{B}_1$ has been turned on for the same duration as in (b).

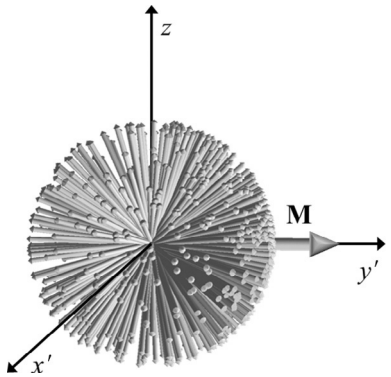

FIGURE 2.16 The spin ensemble after an on-resonance 90° pulse in the rotating frame.

in a rotating frame. As far as T_2 relaxation is concerned, we do not have much of a problem, since the weak interaction among spins will disperse them evenly in the (x',y') plane according to the statistical considerations outlined above, irrespective of whether we are in a static or a rotating frame. However, the situation with T_1 relaxation is less evident: because in the rotating frame $\mathbf{B}_0$ is formally compensated by the $\boldsymbol{\omega}_D/\gamma$ term to give $\mathbf{B}_0 + \boldsymbol{\omega}_D/\gamma = 0$, *apparently* there is no external magnetic field *felt* by the spins in the rotating frame that would polarize them toward the z axis. In that context, how can we thus explain T_1 relaxation in the rotating frame? Quite often, even seasoned NMR experts become perplexed when confronted with this very basic question. One way to rationalize the fact that T_1 relaxation still "works" in the rotating frame is to treat the relaxation terms (2.20a) and (2.21a) as vectors[9] according to the definitions

$$\mathbf{R}_1 = \frac{\mathbf{M}^{eq} - \mathbf{M}_z}{T_1}, \tag{2.33}$$

$$\mathbf{R}_2 = -\frac{\mathbf{M}_{xy}}{T_2}. \tag{2.34}$$

which may be visualized as shown in Fig. 2.17.

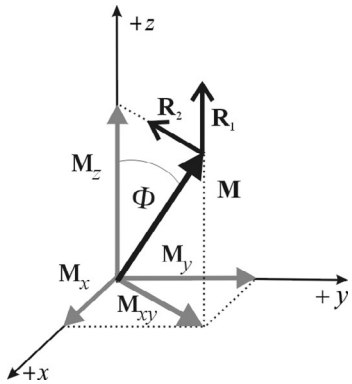

FIGURE 2.17 The relaxation vectors.

Upon transformation into the rotating frame (2.34) remains unchanged except for writing $\mathbf{M}_{x'y'}$ instead of $\mathbf{M}_{xy}$. Thus, T_2 relaxation, as driven by the $\mathbf{R}_2$ vector, takes place just as in the laboratory frame. More importantly however, we immediately see that $\mathbf{R}_1$ is not affected by the transformation Eqs. (2.21a) and (2.21b). This invariance of $\mathbf{R}_1$ to transforming it into the rotating frame ensures that relaxation will progress exactly as in $\mathbf{B}_0$ in the laboratory frame, and that having reached the equilibrium condition $M_z = M^{\text{eq}}$, $\mathbf{R}_1$ vanishes.

There are now a few more points left to be mentioned in preparation of the forthcoming chapters.

One of the greatest strengths of NMR spectroscopy lies in its capability to manipulate spins by using various forms of RF excitation, which allows us to obtain diverse and detailed information on molecular structure (see Chapter 7). Below I will briefly mention three basic forms of RF excitation: (A) the "hard" pulse; (B) the "soft" pulse; and (C) continuous excitation.

(A) The most basic form of hard pulse is a short, rectangular, monochromatic RF pulse which is applied physically as a harmonically oscillating magnetic field of the form $2B_1 \sin(\omega_D t + \varphi)$. As mentioned above, this wave can, as far as its influence on the spins or the **M** magnetization is concerned, be regarded as a $\mathbf{B}_1$ field vector rotating in the (x,y) plane in the same sense as the Larmor precession occurs in the $\mathbf{B}_0$ field (this statement has its own intriguing subtleties, as will be detailed in Chapter 5). The adjective "hard" refers to the fact that the B_1 amplitude, and therefore the angular frequency $\omega_1 = \gamma B_1$, are large enough so that a 90° flip angle is achieved on the order of a few microseconds according to Eq. (2.32). If we have a sample that is more "complicated" than water in the sense that it has several different spin ensembles that each give their own net magnetization **M** such that these magnetizations exhibit different Larmor frequencies, then because the B_1 amplitude is sufficiently large, it can excite a broad range of Larmor frequencies nearly uniformly, that is, the different **M** magnetizations behave nearly as that shown in Fig. 2.15b (this phenomenon will be further elaborated in Chapter 4). As discussed in connection with Figs. 2.16 and 2.17, immediately after the pulse the **M** magnetization is not in equilibrium with the lattice, and therefore it returns back onto the z axis in a process that is determined by three influences: (a) T_1 relaxation restores M_z to its equlibrium value $M_z = M^{\text{eq}}$ according to Eqs. (2.21a) and (2.21b); (b) T_2 relaxation restores M_{xy} to its equilibrium value $M_{xy} = 0$ according to Eqs. (2.22a) and (2.22b); and (c) **M** precesses about the z axis with frequency $\boldsymbol{\omega}_0 = -\gamma \mathbf{B}_0$ under the influence of the torque $\mathbf{M} \times \mathbf{B}_0$ according to Eq. (2.29). The motion of **M** under the combined influence of these factors following a 90° pulse that is assumed to have tilted **M** down to the y axis of the laboratory fame is shown in Fig. 2.18.

If we look at the projection onto the (x,y) plane of the spiral path traced by the tip of **M** in Fig. 2.18 as a function of time such that we commence observation at time $t = 0$ right after the pulse has been turned off, we see a damped harmonic oscillation which decays with a time-constant T_2, as shown for the M_y component in Fig. 2.19a.

In an RF coil designed such as to detect the M_{xy} component, this oscillating magnetization will induce, according to Faraday's law of induction, a voltage which can be received in the form of a signal, called the free induction decay (FID), that corresponds to Fig. 2.19a. The spectrum is obtained by the Fourier transform (FT) of the FID which converts the temporal signal into a frequency-dimension signal (Fig. 2.19b). Because of the exponentially

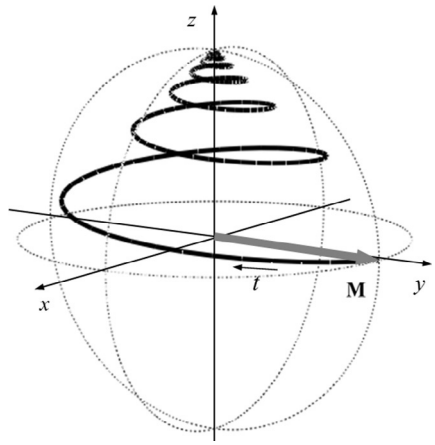

FIGURE 2.18 Return of the **M** magnetization to equilibrium following a 90° pulse.

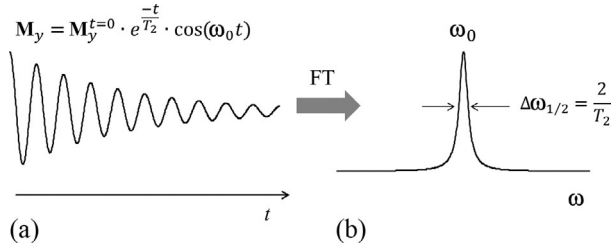

FIGURE 2.19 The detected temporal signal (a) and its Fourier-transformed spectrum (b).

decaying form of the FID, the resonance signal of the spectrum has a Lorentzian shape with a peak maximum at the Larmor frequency ω_0, and a half-width at half-height $\Delta\omega_{1/2} = 2/T_2$ (in reality ω_0 is measured relative to a suitable reference frequency).

For a sample which has, say, two equilibrium macroscopic magnetizations $\mathbf{M}_A^{eq}$ and $\mathbf{M}_B^{eq}$ due to two different spin ensembles (such as, e.g., in the case of a 1:1 molar mixture of dimethyl ether and acetone), upon having tilted these magnetizations away from their equilibrium position, they will precess about the z axis with different Larmor frequencies ω_{0A} and ω_{0B}. Using a hard pulse whose frequency ω_D is not too far from ω_{0A} and ω_{0B}, we can flip the magnetizations simultaneously, in which case the FID obtained after the pulse will be the superposition of the individual FID-components due to M_{xyA} and M_{xyB} (Fig. 2.20), and so the spectrum resulting from the FT of the FID (Fig. 2.20c) will give both resonance frequencies from one experiment.

Besides the capability associated with RF pulses to manipulate spins in wonderfully innovative and useful ways (see Chapter 7), one of the main practical advantages of using hard-pulse excitation is the convenient possibility to increase the spectral signal-to-noise ratio (S/N) through the process of spectral accumulation, which is of primary importance because of the inherent insensitivity of NMR. As a result of this insensitivity, the detected resonance signal is relatively small as compared to the electronic noise of the spectrometer. During accumulation several pulses are applied in a row by allowing sufficient time between two consecutive pulses for the spin ensemble to relax; the FIDs are recorded after

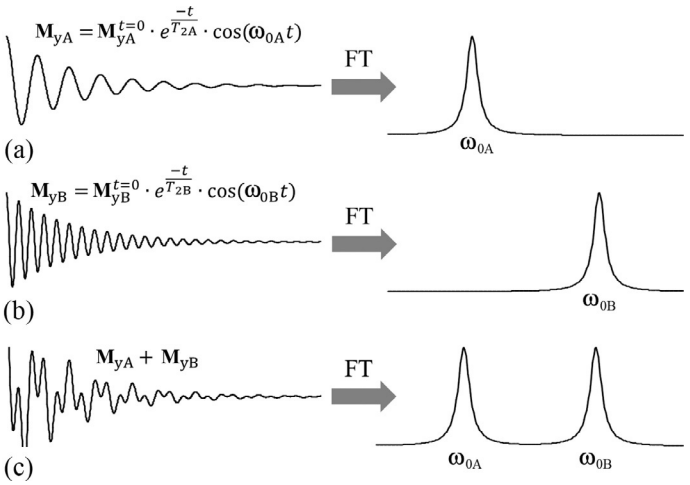

FIGURE 2.20 The FID detected as a superposition (c) of two FIDs with different Larmor frequencies (a) and (b) and their Fourier-transformed spectra.

each pulse and summed before the FT is performed. Because at each resonance frequency the noise level varies randomly after each individual pulse, but the resonance signal "stays put," by adding (accumulating) several spectra originating from a number of consecutive pulses the S/N ratio will increase with the square root of the number of pulses: $S/N \propto \sqrt{\text{number of pulses}}$. Because a hard pulse together with relaxation takes only a few seconds, pulsed excitation offers a handy means for accumulation.

(B) In the case of a "soft" pulse, we employ an RF driving field with a much smaller B_1 amplitude but over a longer duration which is on the order of 10 ms (this is still very short relative to typical T_1 and T_2 relaxation times). With soft pulses one may excite a narrow frequency range or even just a single selected resonance within the whole spectrum. Soft pulses are typically not rectangular but can have a variety of shapes that are tailored to give different excitation profiles. Shaped soft pulses play an important practical role in the so-called selective measurement techniques (see Chapter 7).

(C) In a continuous-wave (CW) RF excitation we again use a wave of the form $2B_1 \sin(\omega_D t + \varphi)$ with a constant but weak amplitude over a time which is on the order of T_1 and T_2. The most typical purpose of such an irradiation is to quench the macroscopic magnetization of a given spin ensemble within the spectrum while leaving other spin ensembles unaffected. More specifically, the purpose of such a Larmor-frequency-selective irradiation is to achieve a state close to that shown in Fig. 2.9a even though the spin ensemble is in the $\mathbf{B}_0$ field, so that $M_z \approx 0$, and also $M_{xy} \approx 0$. In NMR terminology, such a condition is called a *saturated* state which has many practical uses, such as when suppressing large solvent signals or investigating chemical exchange phenomena or dipolar spin-spin interactions—see Chapter 7. The transient process through which saturation is achieved is shown in Fig. 2.21: under the influence of a resonant CW irradiation with a $\mathbf{B}_1$ field employed along the $+x'$ axis in the rotating frame, the $\mathbf{M}$ magnetization keeps precessing in the (z,y') plane about the $\mathbf{B}_1$ field while its magnitude decreases until a steady state is reached in which the torque $\mathbf{M} \times \mathbf{B}_1$ that tilts $\mathbf{M}$ toward the y' axis becomes balanced by relaxation.

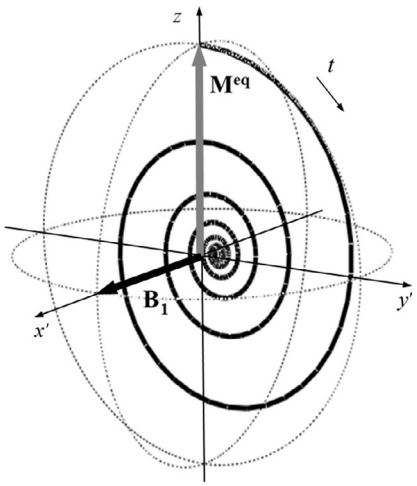

FIGURE 2.21 The transient process of achieving saturation in a continuous $\mathbf{B}_1$ field.

Note that in the "saturated" steady state neither M_z nor $M_{y'}$ can be exactly zero, only a small finite value. In fact, full saturation by this approach can only be achieved in the theoretical limit of $B_1 \to \infty$, in which case $M_z \to 0$, $M_{y'} \to 0$. The nature of this steady-state condition can be understood by considering again the relaxation vectors $\mathbf{R}_1$ and $\mathbf{R}_2$ as defined by Eqs. (2.33) and (2.34). Let us also define a total relaxation vector $\mathbf{R}$ as

$$\mathbf{R} = \mathbf{R}_1 + \mathbf{R}_2 \tag{2.35}$$

and let us remind ourselves of our assumption that $T_1 = T_2$. As it follows from the definition of (2.35) and the underlying definitions (2.33) and (2.34), if $\mathbf{M}$ has been tilted away from the z axis by an angle Φ, the $\mathbf{R}$ vector always points toward the tip of the $\mathbf{M}^{eq}$ vector. If for simplicity we take both T_1 and T_2 to be unity, then we have $\mathbf{R} = \mathbf{M}^{eq} - \mathbf{M}$ as shown in Fig. 2.22. If the $\mathbf{B}_1$ field is

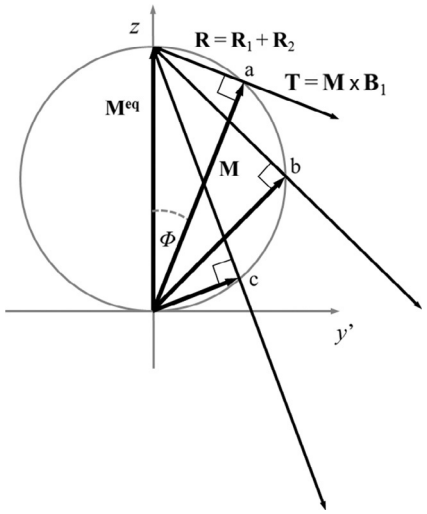

FIGURE 2.22 The steady-state condition of (semi) saturation achieved in a continuous $\mathbf{B}_1$ field employed along the $+x'$ axis in the rotating frame. The points a, b, and c represent steady-state conditions corresponding to increasing B_1 field amplitudes, which results in smaller M_z magnetizations, that is, the degree of saturation increases. In each steady-state point the torque vector $\mathbf{T} = \mathbf{M} \times \mathbf{B}_1$ balances the relaxation vector $\mathbf{R} = \mathbf{R}_1 + \mathbf{R}_2$. With increasing B_1, the tip of $\mathbf{M}$ moves along a Thales circle if $T_1 = T_2$.

continually turned on along the $+x'$ axis in the rotating frame, then in essence we end up with a steady-state situation in which the torque $\mathbf{T} = \mathbf{M} \times \mathbf{B}_1$ keeps "pushing" $\mathbf{M}$ toward the $+y'$ axis, while the $\mathbf{R}$ vector keeps "pulling" it back toward the state corresponding to $\mathbf{M}^{\text{eq}}$. Because $\mathbf{T}$ is perpendicular to $\mathbf{M}$, the steady-state condition $\mathbf{T} + \mathbf{R} = 0$ ensures that $\mathbf{R}$ must also be perpendicular to $\mathbf{M}$. Thus, when, by using larger B_1 fields we increase the torque $\mathbf{T} = \mathbf{M} \times \mathbf{B}_1$ and thereby we force $\mathbf{M}$ to take up larger Φ values, $\mathbf{M}$ will move along a Thales circle in the (z,y') plane.[8] Thus, the larger the B_1 field, the smaller M_z becomes, therefore the greater the degree of saturation will be.

2.5 PRELIMINARY COMMENTS ON THE QUANTUM-MECHANICAL DESCRIPTION OF MAGNETIC RESONANCE

The quantum-mechanical principles that pertain to the NMR phenomenon, as well as a number of false myths which have become quite prevalent in the NMR community and stem from a misunderstanding of those principles or from their unjustified combination with classical concepts, will be discussed in Chapter 3. Nevertheless, a few preliminary comments leading from the above classical considerations to the forthcoming discourse, with our spin ensemble of spin-1/2 nuclei in mind, are due here.

As is almost universally discussed in the basic NMR literature, in a $\mathbf{B}_0$ field the μ magnetic moment of a *single* isolated spin-1/2 nucleus (which is not a member of a spin ensemble), when measured in the direction of the field (i.e., the z direction in our usual Cartesian frame), will give one of two possible discreet values, namely, $\mu_z = +(1/2)\gamma\hbar$ or $\mu_z = -(1/2)\gamma\hbar$, where h is Planck's constant and $\hbar = h/2\pi$. Accordingly, a spin can have two possible energy values, $E_\mu^{\text{pot}} = -(1/2)\gamma\hbar B_0$ or $E_\mu^{\text{pot}} = +(1/2)\gamma\hbar B_0$ (cf. Eq. 2.3). This is the basis of the concept that a spin, if treated as a vector, can have two quantum states, one in which it points "up," that is, toward the $\mathbf{B}_0$ field, which is called the α state, and one in which it points "down," that is, opposite to the $\mathbf{B}_0$ field, which is called the β state.

These considerations lead to the widely held idea that if we take a spin ensemble of noninteracting or weakly interacting spins, the ensemble behaves just as a single spin would, except for being multiplied by the number of spins in the ensemble. Accordingly, the ensemble is viewed as exhibiting two energy levels (the Zeeman levels) with energies $E_\alpha = -(1/2)\gamma\hbar B_0$ and $E_\beta = +(1/2)\gamma\hbar B_0$, and so the energy difference is $\Delta E = \gamma\hbar B_0 = \hbar\omega_0$. At any given time, the spins are inferred to be in either of the two states, with the number of spins populating the α and β energy levels being N_α and N_β, respectively. According to this scenario, the population difference N_α–N_β is proportional to the longitudinal macroscopic magnetization M_z. At thermal equilibrium with the lattice, there are slightly more spins populating the α state than the β state and $(N_\alpha - N_\beta) \propto M^{\text{eq}}$. In this case, the population ratio is determined by Boltzmann's formula so that $N_\alpha/N_\beta = \exp(-\gamma\hbar B_0/kT) = \exp(-\Delta E/kT)$.

This two-level image is not only a vintage model of magnetic resonance, but also a rather convenient one for many purposes. For example, it readily lends itself to viewing the resonance phenomenon as transitions between the two energy levels. These transitions can be induced by irradiation with an electromagnetic field whose frequency satisfies the condition $\Delta E = \gamma\hbar B_0 = \hbar\omega_0$, that is, if $\omega_0 = \gamma B_0$, which is just the formula for Larmor precession discussed above (Eq. 2.8).

The two-level concept seems to be consistent with other forms of spectroscopy (such as UV, IR) which are all based on the phenomenon that electromagnetic waves can interact with

matter such that the latter absorbs an energy quantum (a "photon" with energy $\hbar\omega_0$) from the wave, while some physical feature of the matter undergoes a transition between two quantum states whose energy difference corresponds with $\hbar\omega_0$ (such as electronic quantum states in the case of UV and vibrational quantum states in the case of IR).

The two-level formalism of magnetic resonance offers a correct mathematical treatment of such NMR phenomena that can be treated in terms of rate equations describing the transition of spins between the α and β energy levels. For example, it is well suited to treat relaxation phenomena by using the concept of transition probabilities. During the dynamic energy exchange between the spin ensemble and the lattice an "upward," that is, energy-gaining spin transition between the α and β states can induce a "downward," that is, energy-losing transition of the molecule from a higher rotational quantum state to a lower state, such that the energy difference between the spin energy levels and the lattice energy levels is the same. The probability of an $\alpha \rightarrow \beta$ spin transition induced by this interaction can be characterized by the probability constant $W_{\alpha\rightarrow\beta}$ which denotes the number of $\alpha \rightarrow \beta$ transitions occurring for a unit number of α spins in unit time. The same applies to the reverse process, of course, and so the reverse transition probability constant is $W_{\beta\rightarrow\alpha}$. Thus, at any given time the "upward" spin flux is given by the product $N_\alpha W_{\alpha\rightarrow\beta}$, while the downward spin flux is given by $N_\beta W_{\beta\rightarrow\alpha}$. The same statistical considerations can be applied to this model of the spin-lattice interaction as discussed in Section 2.4. These considerations also lead to the result that at thermal equilibrium, in which case $N_\alpha W_{\alpha\rightarrow\beta} = N_\beta W_{\beta\rightarrow\alpha}$, N_α must be slightly larger than N_β in order for the number of microstates of the combined spin-lattice system to be the maximum, that is, $W_{\beta\rightarrow\alpha} > W_{\alpha\rightarrow\beta}$.

Saturation can also be easily conceptualized in terms of the two-level model. In the interaction of the spin ensemble with the RF irradiation we have upward and downward transition probability constants $P_{\alpha\rightarrow\beta}$ and $P_{\beta\rightarrow\alpha}$ for which it can be proved that $P_{\alpha\rightarrow\beta} = P_{\beta\rightarrow\alpha}$. Thus, if relaxation were not present, under the influence of a continuous RF irradiation the steady-state condition $N_\alpha P_{\alpha\rightarrow\beta} = N_\beta P_{\beta\rightarrow\alpha}$ would mean that $N_\alpha = N_\beta$, that is, the two levels would become equally populated (saturated), giving $M_z = 0$. In reality relaxation of course works against saturation as described above, so steady state will correspond to the condition $N_\alpha(P_{\alpha\rightarrow\beta}+W_{\alpha\rightarrow\beta}) = N_\beta(P_{\beta\rightarrow\alpha}+W_{\beta\rightarrow\alpha})$. These concepts typically form the basis of treating several phenomena that are important in NMR, such as saturation transfer and the NOE.[10]

The two-level concept of spins also offers a convenient and intuitively convincing way of explaining the phenomenon of *J*-coupling: if two spins, *j* and *k*, are separated by only a few chemical bonds, they will sense each other's "up" or "down" orientation as transmitted by the electrons of these bonds. Thus, if spin *k* is "up," this will add a very tiny bit of magnetic field to the main magnetic field experienced by *j*, while if spin *k* is "down," this will very slightly decrease the magnetic field experienced by *j*. As a result, *j* will exhibit two, very slightly different Larmor frequencies, and its resonance signal will accordingly be split into two parts.

In all, the two-level portrayal of magnetic resonance seems to be a rather appealing model. It gives accurate predictions regarding several NMR phenomena, and treats magnetic resonance directly at the quantum-mechanical level without trying to "force" classical-mechanical equations upon the quantum world. All this lends to the two-level model an air of credibility that seems to surpass that of the classical description.

A pictorial extension of this model that attempts to accommodate phenomena involving the transverse component of either the magnetic moment vector or the macroscopic

magnetization, such as Larmor precession, T_2 relaxation, or the tilting of the macroscopic magnetization $\mathbf{M}$, is the famous double-cone model. In this model, an ensemble of $N_\alpha + N_\beta$ spins is envisaged in the $\mathbf{B}_0$ field as N_α spins Larmor-precessing in unison on a cone aligned along the z axis (as in Fig. 2.2) so that the spins are scattered evenly within the transverse plane; this cone represents the α state. On the other hand, N_β spins are Larmor-precessing similarly on a cone pointing in the opposite direction, representing the β state. The two cones have a common apex in the origin. This double-cone image of a spin ensemble is so widely accepted that it has become an almost iconic symbol of NMR spectroscopy.

Both the two-level model and the double-cone picture are in sharp contrast with the classical description of a spin as discussed in Section 2.3, and the "hedgehog" image of a spin ensemble shown in Figs. 2.9 and 2.16. This raises the question: wherein lies the truth?

As argued in Chapter 1, Pillar 3, there is no such thing as absolute truth in science, only an approximation of that truth by a suitable description. That description may be sound or unsound (Pillar 13), it may reflect different levels and modes of understanding (Pillar 6), and the same phenomenon can be described by quite different models (Pillar 13). However, no matter how philosophical we chose to be about the gray-zone nature of scientific truths, and no matter how liberally we can switch our thinking from one model to another, this discrepancy between the "hedgehog" and the two-level picture of a spin ensemble is certainly not something that can go unresolved, because these descriptions paint completely different pictures of the same physical reality. This issue will be unfolded in Chapter 3. However, in order to substantiate the validity of the classical description outlined above so as to wrap up this chapter without having to leave this discrepancy lingering, suffice to point out here briefly the following items.

Unlike in optical spectroscopy, in NMR the resonance signal is *not* caused by radio-frequency electromagnetic photons of $\hbar\omega_0$ energy being absorbed by the spin ensemble, and NMR relaxation is *not* a process of emitting those photons whilst the spins return from an "excited" state to a "nonexcited" state. Rather, the NMR signal is induced by a purely magnetic interaction between the driving $\mathbf{B}_1$ field and the magnetic moments (or the macroscopic magnetization, if you will) and during NMR relaxation the energy released by the spin ensemble passes into the lattice in the form of a tiny amount of heat as was described earlier. This topic was brought to light and thoroughly explored in a series of wonderful papers by David Hoult.[11–13]

The two-level model of a spin ensemble gives accurate predictions within the model's contextual space (cf. Pillar 13), that is, for several important NMR phenomena whose treatment focuses on the M_z magnetization and requires only rate equations as discussed above. However, many NMR phenomena fall outside the contextual space of the two-level formalism, for example, the transversal magnetization generated by, say, a simple 90° pulse, cannot be described by the two-level rate equations, and in that regard the model fails. The point that I want to make from this is that although *within* its contextual space the two-level model gives valid predictions *mathematically*, it is a misleading representation of the *physical* world. In reality, deeper quantum-mechanical considerations tell us that spins in a spin ensemble placed in a $\mathbf{B}_0$ field do *not* exist in a pure α or β state, but in a mixed, or so-called *superposition* state, of which one may think of as a spin being simultaneously to some extent in an α, and to some extent in a β state. As will be more fully explained in Chapter 3, this quantum-mechanical mixing of the two states leads not to a simple vector-addition of the "up" and "down"

α and β spin vectors as one might intuitively expect, but to the "mixed" spins becoming oriented in *any* direction in space. It may be worth pointing out that a spin being in a superposition state of the α and β states is *not* the same thing as having a probability of being in either.

Thus, according to the physically correct quantum-mechanical picture, spins are actually distributed in a 3D *spin space* in a manner which is analogous to the spin-globe expected classically as shown in Fig. 2.9. This feature of the spins was pointed out by several authors in NMR—see, for example, Refs. 1,5,7,14. As noted by Slichter:

> "We emphasize that an *arbitrary* orientation can be specified, since sometimes the belief is erroneously held that spins may only be found pointing either parallel or antiparallel to the quantizing field. In terms of the two quantum states α and β we can describe an *expectation* value of magnetization which may go all the way from parallel to antiparallel, including all values in between."[14]

As it happens, the expectation value for a single spin that is a part of the spin ensemble obeys the equation $d\langle\boldsymbol{\mu}\rangle/dt = \langle\boldsymbol{\mu}\rangle \times \gamma\mathbf{B}$, which is just the classical equation of motion (2.5). Because the experimentally measured net magnetization $\mathbf{M}$ is simply the expectation value of the total magnetic moment, the classical equation correctly describes the dynamics of $\mathbf{M}$.[14] Indeed, it should be appreciated that a complete quantum-mechanical description of magnetic resonance describes vector dynamics, not just rate equations as the simple two-level picture implies.

Although the two-level picture does not represent physical reality appropriately, the fact that calculations based on this picture give good predictions under many circumstances is however no coincidence. This is because with regard to the quantum-mechanically calculated behavior of the spins, in those circumstances it is irrelevant whether the spins are oriented arbitrarily within a spin-globe of mixed states, or are only in pure α and β states. Thus we may say that, according to the considerations and terminological definitions discussed in Pillar 13, the two-level model is mathematically sound in the sense that it gives accurate predictions, but physically unsound in the sense that it misrepresents physical reality. The widespread misunderstanding of the two-level model is due mainly to Traps #7, #8, #10, #11, and #18: because of its broad and traditional acceptance, its intuitive appeal, as well as its good predictive power, the two-level picture is easily mistaken for physical reality (note, e.g., that the Larmor formula $\omega_0 = \gamma B_0$ derived above from the two-level picture is the same as that inferred from classical considerations, and this identity can be easily interpreted as a physical validation of the two-level model).

The double-cone model is however an unsound metaphoric pictorial model, that is, a Delusor, in every respect: It does not serve the purpose of quantitative predictions and is entirely inconsistent with physical reality, especially when it is used to explain the motion of $\mathbf{M}$ during or following excitation by a $\mathbf{B}_1$ field. The reason why it has become an iconic entity in NMR is again clearly due to its intuitively appealing nature and the preconceived knowledge that it is a universally accepted "truth." All this creates a strong emotycal support for this model, which can block people's incentive to "scratch below the surface." This is all the more interesting because the double-cone model carries serious and almost glaringly obvious internal inconsistencies (see Chapter 3) which are simply skipped over by many people (see the concept of emotycal heuristic mentioned in Pillar 4), although these could be easily discovered by directing one's Rational Mind to the problem.

J-coupling is a particularly intriguing topic with regard to the two-level versus "hedgehog" picture of spins: while it can be very easily explained, and formally correctly treated in terms of the two-level model, it is at first sight far less obvious how *J*-coupling can be rationalized with either the quantum-mechanical or the classical "hedgehog" model. Since the two-level description is not a faithful representation of physical reality, this situation can again create an uncertainty in one's mind as to "wherein lies the truth." In fact, *J*-coupling *can* be understood classically if one treats the *j* and *k* spin as a system of coupled pendulums[1] (see somewhat more on this in Chapter 3).

As stated previously, the above very cursory foray into the quantum-mechanical world of NMR served the purpose of putting the classical description offered in this chapter in the context of the quantum-mechanical concept of the behavior of spins in a magnetic field, as well as to serve as a thematic bridge toward the next chapter. Chapter 3 will discuss the above items in proper detail.

2.6 SUMMARY

In this chapter, I attempted to give an introductory discourse on some fundamental aspects of the NMR phenomenon by mainly focusing on a classical description at a "synoptic" level (Pillar 6). I also injected some elements of AA into this treatment, particularly by trying to sensitize the discussion toward approaching NMR in a model-conscious frame of mind (Pillar 13, Trap #18) and toward differentiating between our mathematical and physical understanding of the world (Pillar 6). With this standpoint in mind, I tried to offer a view of the behavior of spins in a magnetic field in terms of some statistical considerations pertaining to relaxation and by drawing an analogy with rigid-body dynamics for the understanding of the resonance phenomenon itself. In their present form, such descriptions are rarely found in the NMR literature. The approach to treat spins in a classical manner is initially clearly based on a heuristic (in a scientific sense) assumption since we know that spins are quantum-mechanical entities that give quantized magnetic moments in a magnetic field. Nevertheless, deeper quantum-mechanical considerations (not discussed here) show that the classical approach gives a physically sound model within its contextual space (Pillar 13). I also made some brief comments on the quantum-mechanical approach to NMR in order to place the classical description in context without which this chapter could not have been reasonably self-contained. There are some widespread misconceptions about the physical essence of NMR stemming from a naïve and emotycs-driven understanding of what quantum mechanics tell us about the behavior of spins. These will be discussed in Chapter 3. All this shows that even some 70 years after laying down the theoretical and experimental foundations of NMR, there are still issues to be clarified and ongoing arguments about the proper physical interpretation of the NMR phenomenon, highlighting the need to always keep looking backward (Pillar 17) in a quest of searching for scientific "truth" (Pillar 3).

Acknowledgments

I am grateful to Dr. Zsuzsanna Sánta and Dr. Lars Hanson for their very helpful comments.

References

1. Hanson LG. Is quantum mechanics necessary for understanding magnetic resonance? *Concepts Magnetic Reson* 2008;**32**:329–40.
2. Bloch F. Nuclear induction. *Phys Rev* 1946;**70**:460–74.
3. Purcell EM, Torrey HC, Pound RV. Resonance absorption by nuclear magnetic moments in a solid. *Phys Rev* 1946;**69**:37–8.
4. Rigden JS. Quantum states and precession: the two discoveries of NMR. *Rev Mod Phys* 1966;**58**:433–48.
5. Levitt MH. *Spin dynamics. Basics of nuclear magnetic resonance.* 2nd ed. Chichester: Wiley; 2011.
6. Rabi II, Ramsay NF, Schwinger J. Use of rotating coordinates in magnetic resonance problem. *Rev Mod Phys* 1954;**26**:167–71.
7. Corio PL. *Structure of high-resolution NMR spectra.* New York: Academic Press; 1966, (a) p. 26. (b) p. 63–4.
8. Reif F. *Fundamentals of statistical and thermal physics.* Reissue, Illinois: Waveland Press; 2009.
9. Szántay Jr Cs, Kürti J, Janke F. A simple, geometrical approach to the steady-state solution of the Bloch equations. *Concepts Magn Reson* 1991;**3**:161–70.
10. Neuhaus D, Williamson MP. *The nuclear Overhauser effect in structural and conformational analysis.* 2nd ed. New York: Wiley; 2000.
11. Hoult DI. The magnetic resonance myth of radio waves. *Concepts Magn Reson* 1989;**1**:1–5.
12. Hoult DI, Bhakar B. NMR signal reception: virtual photons and coherent spontaneous emission. *Concepts Magn Reson* 1997;**9**:277–97.
13. Hoult DI. The origins and present status of the radio wave controversy in NMR. *Concepts Magn Reson* 2009;**34A**:193–216.
14. Slichter CP. *Principles of magnetic resonance.* New York: Springer-Verlag; 1978, (a) p. 17. (b) p. 20.